# Supporting Information

## Deciphering the incognito role of water in a light driven proton coupled electron transfer process.

*Senthil Kumar Thiyagarajan, Raghupathy Suresh, Vadivel Ramanan, Perumal Ramamurthy**

National Centre for Ultrafast Processes, University of Madras, Taramani Campus,

Chennai - 600 113, India.

Email: prm60@hotmail.com

# Contents

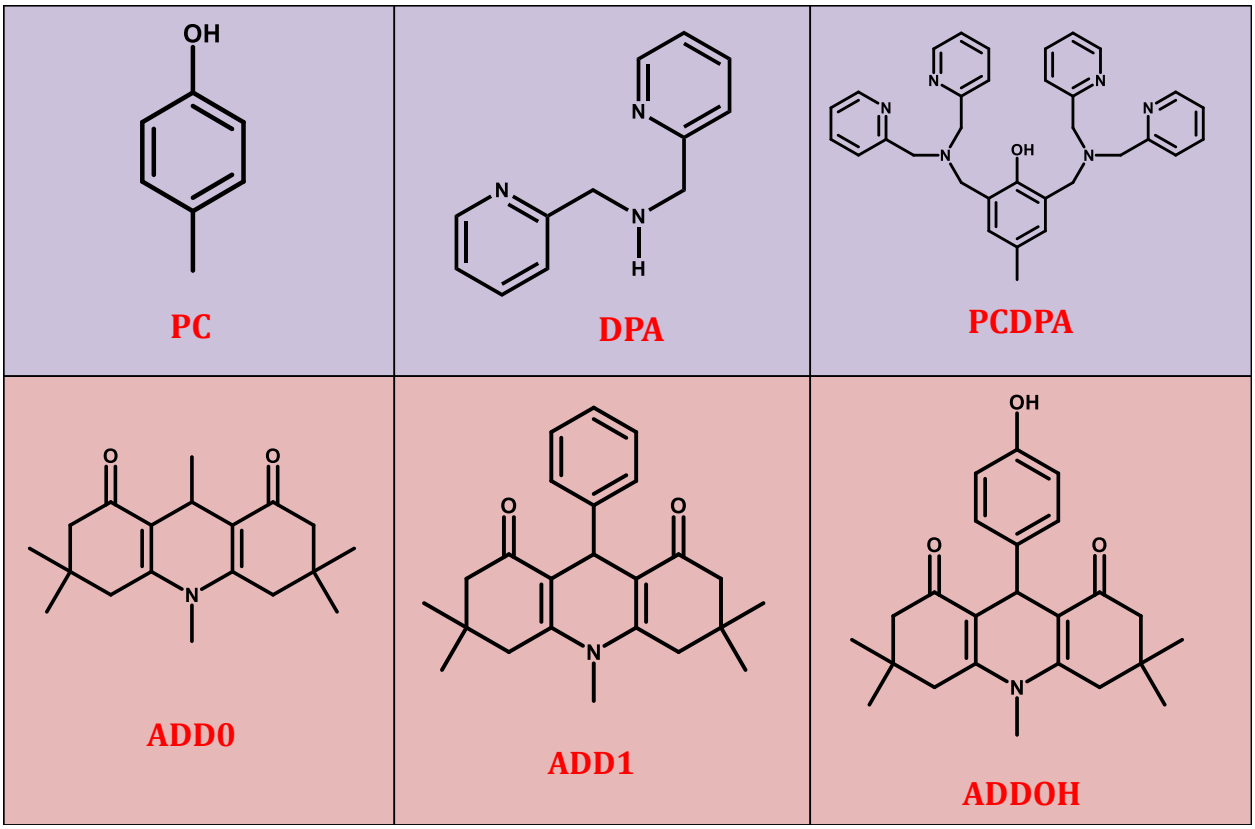


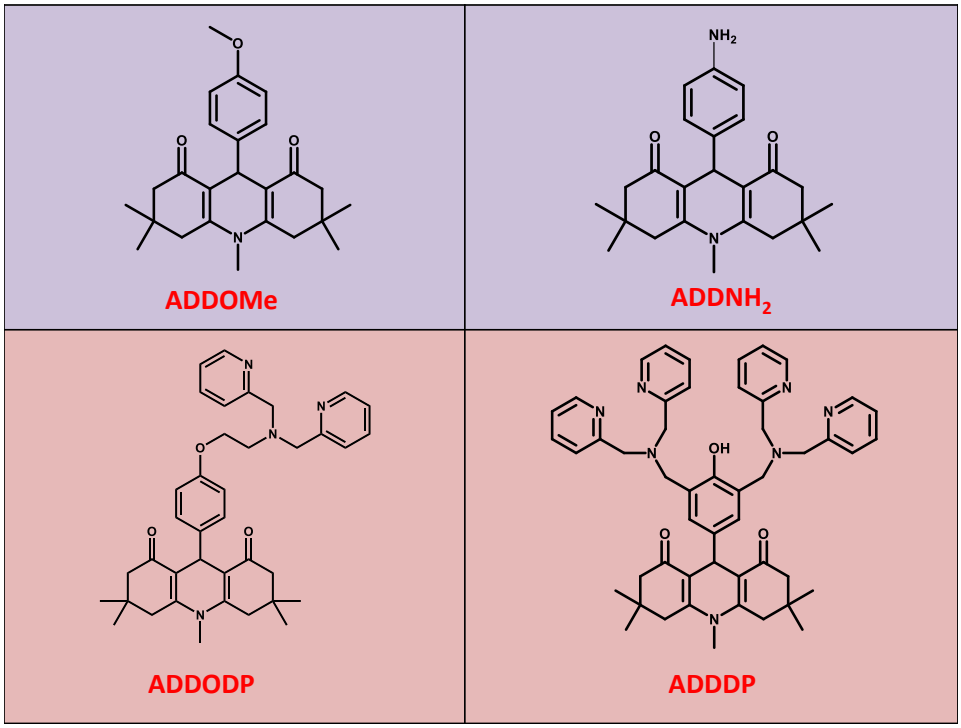


**Molecular structure and name of the compounds used in the present study**

# Abbreviations

| | | |
|---|---|---|
| **NADH** | ➢ | **N**icotinamide **A**denine **D**inucleotide **H**ydride |
| **ETPT** | ➢ | Electron first proton transfer |
| **PCET** | ➢ | **P**roton **C**oupled **E**lectron **T**ransfer |
| **EPT** | ➢ | **E**lectron **P**roton **T**ransfer |
| **MSEPT** | ➢ | **M**ulti**S**ite **E**lectron **P**roton **T**ransfer |
| **CPET** | ➢ | **C**oncerted **T**ransfer of **E**lectron and **P**roton |
| **OEC** | ➢ | **O**xygen **E**volving **C**omplex |
| **ESICT** | ➢ | **E**xcited **S**tate **I**ntramolecular **C**harge **T**ransfer |
| **ESIPT** | ➢ | **E**xcited **S**tate **I**ntramolecular **P**roton **T**ransfer |
| **PET** | ➢ | **P**hotoinduced **E**lectron **T**ransfer |
| **SV plot** | ➢ | **S**tern-**V**olmer plot |
| **TCSPC** | ➢ | **T**ime **C**orrelated **S**ingle **P**hoton **C**ounting |
| **DPA** | ➢ | **D**i**p**icolyl **A**mine |
| **CT** | ➢ | **C**harge **T**ransfer |
| **LE** | ➢ | **L**ocally **E**xcited |
| **TEA** | ➢ | **T**ri**e**thyl **A**mine |
| **DF** | ➢ | **D**eprotonated **F**orm |
| **PF** | ➢ | **P**rotonated **F**orm |
| **NFD** | ➢ | **N**eutral **F**orm with **D**irect hydrogen bonding |
| **NFW** | ➢ | **N**eutral **F**orm with **W**ater mediated hydrogen bonding |
| $k_{ETPT}$ | ➢ | Rate constant of electron first proton transfer |
| $k_{DEPT}$ | ➢ | Rate constant of direct intramolecular electron proton transfer |
| $k_{WMEPT}$ | ➢ | Rate constant of water mediated electron proton transfer |
| $k_{obs}$ | ➢ | Rate constant of observed excited state decay |
| $k_{nr}$ | ➢ | Non-radiative decay rate constant |
| $k_f$ | ➢ | Emissive or radiative decay rate constant |

## Materials

Dimedone and di-(2-picolyl) amine were purchased from Aldrich Chemicals Pvt. Ltd. 4-Hydroxybenzaldehyde, methyl amine and 37% formaldehyde were purchased from Sisco Research Laboratory (SRL). All the chemicals were used as received unless otherwise stated. Solvents used for the photophysical studies were of HPLC grade, purchased from Qualigens India Ltd. Prior to use all the solvents were purified and dried using the standard methods.[1, 2] Analytical grade solvents were used for the synthesis and purification purpose.

## Synthesis and characterization details

### Preparation of 2, 2'-((4-hydroxyphenyl) methylene)bis(5,5-dimethylcyclohexane-1,3-dione) (TKOH).[3]

To a solution of dimedone (2.0 g, 14.26 mmol) in aqueous methanol, 4-hydroxybenzaldehyde was added (0.87 g, 7.13 mmol) and the reaction mixture was warmed until the solution became cloudy. Then the reaction mixture was diluted with water (250 mL) the solid obtained was filtered, dried and recrystallized using methanol. (Yield: 90%) (m.p. above 200$^{o}$C).

### Preparation of 9-(4-hydroxyphenyl)-3,3,6,6-tetramethyl-3,4,6,7,9,10-hexahydro acridine-1,8(2H,5H)-dione (ADDOH).[3]

A mixture of tetraketone (1.0 g, 2.6 mmol) and methyl amine (0.48 g, 15.6 mmol) in acetic acid (20 mL) was kept under reflux for 8 hours. Then the reaction mixture was cooled and poured over crushed ice. The solid obtained was filtered and dried. The compound obtained was purified by silica gel column chromatography and eluted with $CHCl_3$ : MeOH (96:4, v/v) to get the pure ADDOH.(Yield: 83%) (m.p. above 250$^{o}$C). IR (KBr): 3267.08 (br, -OH), 2960.59 & 2869.74 (s, aromatic CH) 1629.25, (s, C=O), 1370.77 (s, -C=C-) cm$^{-1}$. $^{1}$H NMR : 400MHz, DMSO-$d_6$: δ ppm; 0.94 and 0.99 (2s, 12H, gem- dimethyl); 2.06-2.15 (ABq, 4H, methylene proton); 2.38-2.77 (2d, 4H, J=22Hz, methylene proton); 3.25 (s, 3H, N-$CH_3$); 4.91(s, 1H, $C_9$-H) 6.50 - 6.53(d, 2H, J=10.5Hz, Ar-H); 6.85-6.87 (d, 2H, J=10.5Hz, Ar-H); 9.00(s, 1H, O-H). $^{13}$C NMR: 100 MHz, DMSO-d6; δ ppm; 28.22, 28.82, 30.16, 32.61, 33.69, 39.62, 50.04, 113.69, 114.96, 128.44, 137.11, 152.73, 155.61, 195.28. MS (ESI): m/z = 380.43 $[M + 1]^{+}$. $C_{24}H_{29}N_1O_3$ (379.49): calcd. C 75.96, H 7.70, N 3.69; found C 75.85, H 7.66, N 3.64.

**Synthesis of 9-(3,5-bis((bis(pyridin-2-ylmethyl)amino)methyl)-4-hydroxyphenyl)-3,3,6,6-tetramethyldecahydroacridine-1,8(2H,8aH)-dione (ADDDP).**

To a solution of ADDOH (0.5 g, 1.32 mmol) in isopropanol (5mL) and water (5mL) was added di-(2-picolyl) amine (0.58g, 2.90mmol ) and 37% formaldehyde solution (0.16 g, 5.27mmol). The resulting solution was kept under reflux for 12h. Isopropanol was removed from the reaction by vacuo and then 10 mL of water was added. The resulting solution was extracted using ethyl acetate(2 x 10mL) and the organic phase washed with saturated $NaHCO_3$ (2 x 10mL). The combined organic layer was dried over sodium sulphate and evaporated under reduced pressure. Then the crude product was purified by alumina column chromatography ($CHCl_3$–MeOH, 99:1) to yield a yellow solid. After purification the compound was recrystallized using ethyl acetate (Yield: 80%, m.p. 150$^oC$). $^1H$ NMR (400 MHz, $CD_3CN$); $\delta$ = 0.894 and 0.978 (2s, 12H, gem-dimethyl); 1.998-2.162 (ABq, 4H, J = 16 Hz, $C_2$ & $C_7$ -CH2); 2.404-2.447 & 2.633 – 2.676 (2d, 4H, J = 17.2 Hz $C_4$ & $C_5$ -$CH_2$); 3.240 (s, 3H, N-$CH_3$ ); 3.595 (s, 4H, $CH_2$); 3.697(s, 8H, $CH_2$); 4.979 (s, 1H, $C_9$-H); 6.942 (s, 2H, Ar-H); 7.252 – 7.264 (m, 4H, Ar-H); 7.420 – 7.439 (m, 4H, Ar-H); 7.717 – 7.755 (m, 4H, Ar-H); 10.695 (s, 1H, Ar-OH). $^{13}C$ NMR (100 MHz, $CD_3CN$); $\delta$ = 26.81, 27.50, 29.99, 31.81, 32.77, 39.41, 49.36, 53.92, 58.71, 113.51, 116.98, 121.73, 122.61, 123.03, 128.03, 136.18, 148.46, 151.89, 158.89, 194.96. HRMS, m/z = 802.4492 $[M + 1]^+$.

**Preparation of 2,6-bis((bis(pyridin-2-ylmethyl)amino)methyl)-4-methylphenol (PCDPA).[4]**

To a solution of 2, 2'-dipicolylamine (1.15 g, 5.78 mmol) and paraformaldehyde (0.27 g, 9.24 mmol) in the solution ($H_2O$: i-PrOH = 1 : 1 (v/v), 20 mL) was added 1N HCl to adjust pH to 8. After stirring at 80$^oC$ for 30 min, p-cresol (0.25 g, 2.31 mmol) was added and the mixture was kept under reflux for 12 h. The mixture was cooled to room temperature, and then i-PrOH was removed by evaporation. After cooling on ice-bath, the solution was removed by decantation, and the precipitated viscous oil was dissolved in ethylacetate. The solution was washed with saturated $NaHCO_3$ and brine followed by drying over $MgSO_4$. After removal of the solvent under reduced pressure, the residue was purified by column chromatography on basic alumina(hexane/dichloromethane) to give an oil (Yield: 24%).$^1H$ NMR (400 MHz, $CDCl_3$); 2.23 (s, 3H, $CH_3$); 3.87(s, 4H, $CH_2$); 4.21 (2, 8H, $CH_2$) 6.81 (s, 2H, Ar-H); 7.45 – 7.49 (t, 4H, J = 6.4

Hz, Ar-H); 7.64 – 7.66 (d, 4H, J = 8 Hz, Ar-H); 7.97 – 8.01 (m, 4H, Ar-H); 8.70 – 8.71 ( d, 4H, J = 4.4 Hz); 10.695 (s, 1H, Ar-OH). $^{13}$C NMR (100 MHz, $CDCl_3$); δ = 20.36, 56.79, 62.81, 121.95, 122.26, 122.97, 123.25, 129.75, 130.17, 148.83, 153.37, 159.30.

# Methods

## IR Spectrometer

IR spectra were recorded on Thermo Scientific Nicolet iS5 FT-IR spectrometer.

## NMR Spectrometer

$^1$H and $^{13}$C-NMR spectra were recorded on a Bruker 400 MHz instrument. The residual solvent peaks were used as internal standards. Chemical shifts are reported in ppm and coupling constants ($J_{X\text{-}X'}$) are reported in Hz.

## Mass Spectrometer

Bruker Maxis ESI-TOF mass analyser type was used for the HRMS measurements.

## Absorption spectrophotometer

Absorption spectra were recorded using Varian Cary Bio 100 UV-Vis spectrophotometer.

## Fluorescence spectrophotometer

Fluorescence spectral measurements were carried out using Horiba-Jobin Yvon Fluoromax-4P fluorescence spectrometer.

## Determination of Fluorescent quantum yield

Fluorescence quantum yields were obtained from the corrected fluorescence spectra using the expression,

$$\mathbf{\Phi_f = (A_s/A_r)\ (a_r/a_s)\ (n_s/n_r)\ x\ 0.546}$$

where $A_s$ and $A_r$ are the area under the corrected fluorescence spectrum, $a_s$ and $a_r$ are the absorbance at the wavelength of excitation (366 nm), $n_s$ and $n_r$ are the refractive indices of the solvent for the sample and reference respectively. Quinine sulphate in 0.1 N sulphuric acid was used as the reference ($\Phi_f$ of quinine sulphate is 0.546).

### Cyclic Voltammetry

Cyclic Voltammetry (CV) studies were carried using a CHI-620B from CH instruments. Glassy carbon (3 mm dia) was used as the working electrode, $Ag/Ag^+$ was used as the reference electrode and platinum wire was used as the counter electrode. The analyte concentration is 1 mM and that of the supporting electrolyte is 0.1M. Supporting electrolyte is KCl in case of aqueous samples whereas for samples dissolved in acetonitrile the supporting electrolyte is tetrabutylammonium hexafluorophosphate (TBAHFP). The capacity of the sample cell is 10 mL which is covered with a four-holed Teflon cap. All the experiments were carried out at room temperature, and the solutions were purged with argon for 30 minutes prior to measurement.

## Time Resolved Fluorescence Studies

### Time Correlated Single Photon Counting Technique (TCSPC)

Fluorescence decays were recorded by using an IBH time-correlated single-photon counting spectrometer as reported elsewhere.[5] Data analysis was carried out by the software provided by IBH (DAS6) which is based on reconvolution technique using iterative nonlinear least square methods. The quality of the fit is normally identified by the reduced $\chi^2$, weighted residual and the autocorrelation function of the residuals. **Instrument Response Function (IRF) ~ 550 ps.**

### Femtosecond Fluorescence Up-conversion Technique

Femtosecond fluorescence decays were recorded using fluorescence up-conversion technique as reported elsewhere.[6] The fluorescence decays were fitted using a Gaussian shape for the excitation pulse with FWHM of 200 fs. **Instrument Response Function (IRF) ~ 200 fs.**

The femtosecond fluorescence decay was analysed using IGOR software by fixing the longer lifetime component obtained from TCSPC.

### Note

- **All the fluorescence lifetime measurements were carried out for at least three times and error in the fitted lifetime values is well within 5%.**

## Femtosecond Transient Absorption Studies

It is a Ti:sapphire laser (Mai Tai HP, Spectra Physics, USA) centered at 800 nm having pulse width of <100 fs with 80 MHz repetition rate. The amplified laser was split into two in the ratio of 75:25%. The high energy beam was used to convert to the required wavelength (380 and 530 nm) for exciting the sample by using TOPAZ (Prime, Light Conversion). The white light continuum (340−1000 nm) was generated by focusing the part of amplified beam (200 mW) on a 1-mm-thick $CaF_2$ plate which split into two beams (sample and reference probe beams). The sample cell (0.4 mm path length) was refreshed by rotating in a constant speed. Finally, the white light continuum was focused into a 100 μm optical fiber coupled to imaging spectrometer after passing through the sample cell. The pump probe spectrophotometer (ExciPro) setup was purchased from CDP Systems Corp, Russia. Normally transient absorption spectra were obtained by averaging about 2000 excitation pulses for each spectral delay. All the measurements were carried out at the magic angle (54.7°). **The time resolution of the pump−probe spectrometer is found to be about >120 fs**.

### Solution preparation for ACN/Water Studies - ADDOH

The stock solution (0.79 mM) was prepared by dissolving 1.5 mg of ADDOH in HPLC grade freshly dried acetonitrile in a 5 mL standard measuring flask at room temperature. Absorption, emission and fluorescence lifetime (TCSPC) studies were carried out by taking 158 μL of ADDOH from this stock solution and diluted to 5 mL, so that the final concentration was 25 μM.

### Solution preparation for ACN/Water Studies - ADDDP

The stock solution (1.25 mM) was prepared by dissolving 5 mg of ADDDP in HPLC grade freshly dried acetonitrile in a 5 mL standard measuring flask at room temperature. Absorption, emission and fluorescence lifetime (TCSPC) studies were carried out by taking 100μL of ADDDP from this stock solution and diluted to 5 mL, so that the final concentration was 25 μM.

Whereas, the concentration of ADDOH and ADDDP solutions used in femto upconversion studies were 250 μM.

### Solution preparation for pH Studies - ADDOH & ADDDP

Similarly, for pH studies (Absorption, emission and fluorescence lifetime using TCSPC studies) 25µM of ADDOH and ADDDP in MeOH/Water (20:80) mixture were used and for femto upconversion studies 250 µM of ADDOH and ADDDP were used.

- For acidic region the pH were adjusted by using concentrated sulphuric acid.
- For basic region the pH were adjusted by using buffer solution - MeOH/Water (20:80, 10mM buffer solutions).

### Preparation of various pH buffer solutions (pH 7 - 12)

Buffer solutions ranging from 7 - 12 was prepared by mixing appropriate volume of acid (0.1 M) and conjugate base (0.1M). Calculation of the ratio of volume required for various pH buffer solutions was done by Henderson-Hasselbalch equation. The resultant buffer solution (0.1 M) was further diluted to 10 mM and this was used for the fluorescence studies.

- pH buffer solution (7 & 8) – phosphate buffer.
- pH buffer solution (9 –12) – bicarbonate buffer.

## Parameters Used for Steady State Fluorescence Measurements

#### ADDOH - ACN/Water Study

Excitation wavelength = 293 nm; excitation slit (nm) = 3; emission slit (nm) = 2.

#### ADDOH - ACN/ $D_2O$ Study

Excitation wavelength = 321 nm; excitation slit (nm) = 3; emission slit (nm) = 2.

#### pH Studies in MeOH/Water (20:80) – ADDOH

Excitation wavelength = 401 nm; excitation slit (nm) = 4; emission slit (nm) = 3.

#### ADDDP - ACN/Water Study

Excitation wavelength = 324 nm; excitation slit (nm) = 6; emission slit (nm) = 3.

#### ADDDP - ACN/ $D_2O$ Study

Excitation wavelength = 300 nm; excitation slit (nm) = 7; emission slit (nm) = 3.

#### pH Studies in MeOH/Water (20:80) – ADDDP

Excitation wavelength = 401 nm; excitation slit (nm) = 6; emission slit (nm) = 3.

## Parameters Used for Time resolved Fluorescence Measurements

- **Fluorescence decay profile studies - TCSPC technique**

  To record the fluorescence decay profile in the nanosecond regime all the samples were excited at 375 nm and monitored at respective emission maximum of each sample.

- **Fluorescence decay profile studies - Femtosecond upconversion**

  To record the fluorescence decay profile in the picosecond regime all the samples were excited at 400 nm and monitored at 450 nm.

## Parameters Used for Femtosecond Transient Absorption Measurements

- Excitation wavelength = 355 nm, **Pulse width = 120 fs**, Energy = ~2micro Joule/ pulse, Repetition rate = 1.0 KHz, Path length = 0.4 mm, Concentration used = ~1.0 OD in 1mm, Solvents = ACN and ACN+ water mixture.

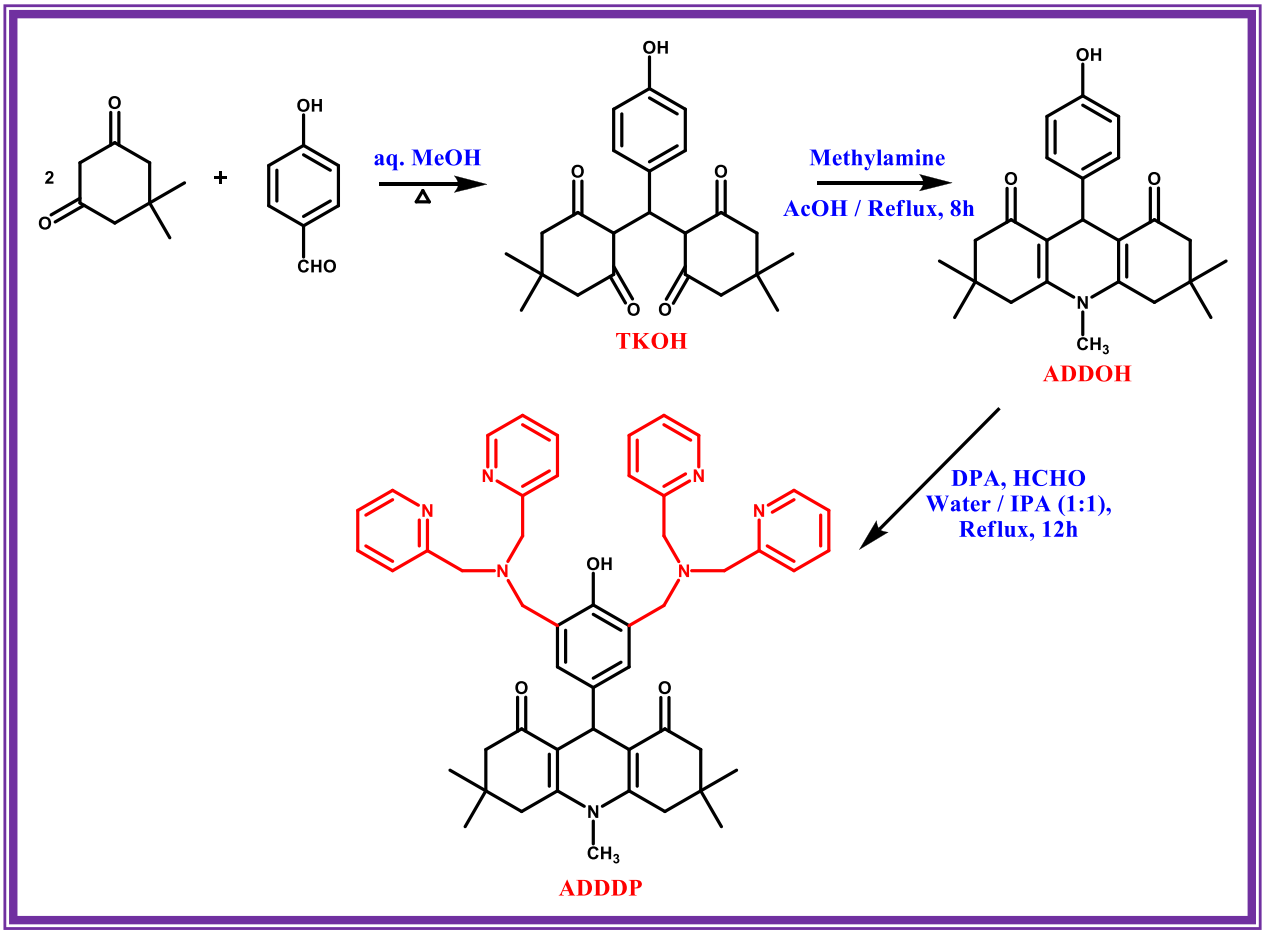


**Scheme S1**. Synthetic scheme of **ADDOH** and **ADDDP.**

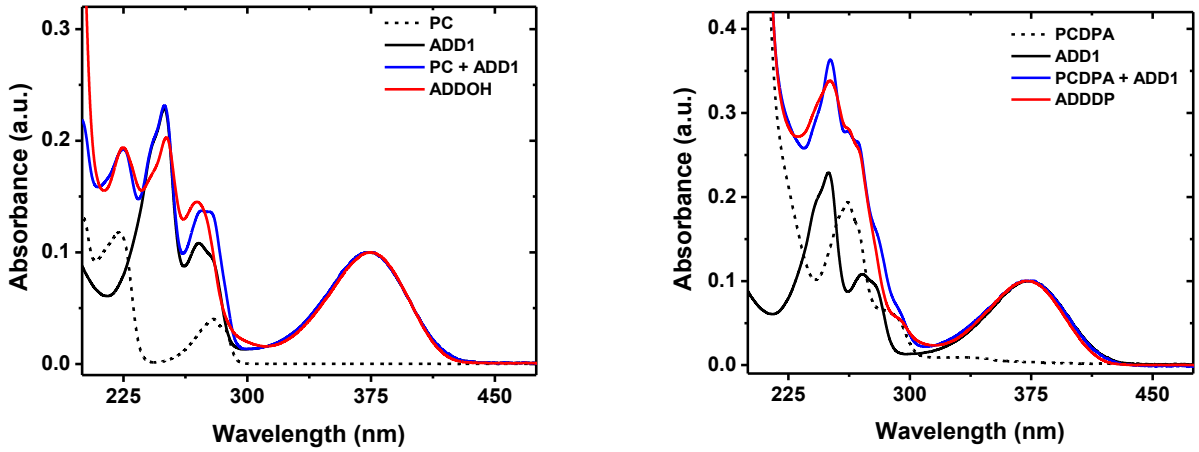


**Figure S1.** Absorption Spectra showing the absence of electronic coupling between the **ADD** moiety and the non-conjugatively pendant phenols.

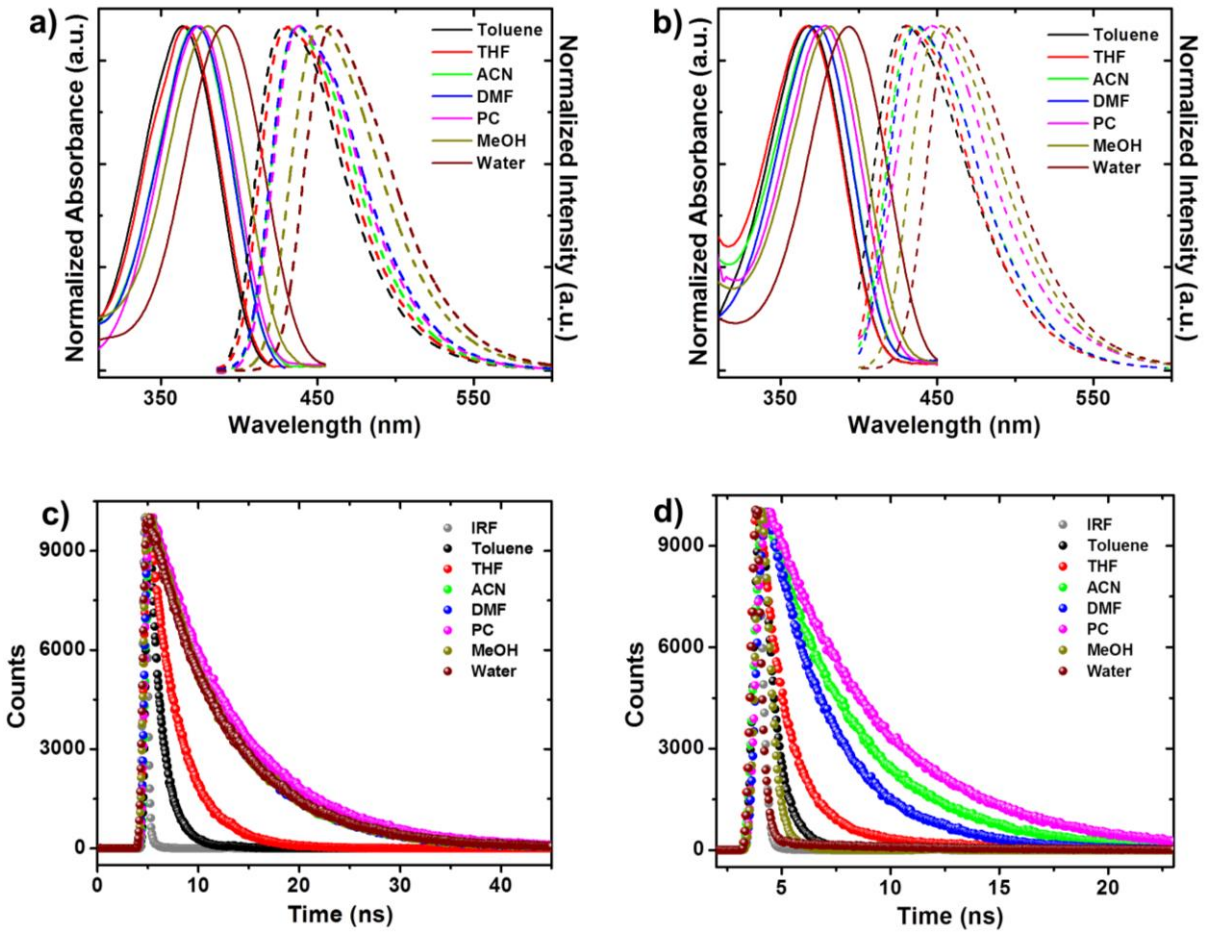


**Figure S2.** Absorption and emission spectra of a) **ADD1** b) **ADDOH** in different solvents, Fluorescence decay profile of c) **ADD1** d) **ADDOH** in different solvents.

**Table S1.** Photophysical data of **ADD1** in different solvents

| Solvent | Abs $\lambda_{max}$ (nm ) | Emi $\lambda_{max}$ nm | Stokes Shift ($cm^{-1}$) | $\phi_f$ | $\tau_f$ (ns) | $k_{total}$ $\times 10^8$ ($s^{-1}$) | $k_f$ $\times 10^8$ ($s^{-1}$) | $k_{nr}$ $\times 10^8$ ($s^{-1}$) |
|---|---|---|---|---|---|---|---|---|
| **Toluene** | 364 | 429 | 4162 | 0.016 | 1.51 | 6.62 | 0.10 | 6.52 |
| **THF** | 366 | 431 | 4121 | 0.138 | 2.91 | 3.44 | 0.47 | 2.97 |
| **ACN** | 373 | 437 | 3926 | 0.567 | 7.37 | 1.36 | 0.77 | 0.59 |
| **DMF** | 373 | 439 | 4031 | 0.570 | 7.45 | 1.34 | 0.76 | 0.58 |
| **PC** | 375 | 439 | 3888 | 0.591 | 8.33 | 1.20 | 0.71 | 0.49 |
| **MeOH** | 380 | 452 | 4192 | 0.505 | 7.39 | 1.35 | 0.68 | 0.67 |
| **Water** | 392 | 460 | 3771 | 0.61 | 7.51 | 1.33 | 0.81 | 0.52 |

**Table S2.** Photophysical data of **ADDOH** in different solvents

| Solvent | Abs $\lambda_{max}$ (nm) | Emi $\lambda_{max}$ (nm) | Stokes Shift ($cm^{-1}$) | $\phi_f$ | $\tau_f$ (ns), A (%) | | $k_{total}$ $\times 10^9$ ($s^{-1}$) | $k_f$ $\times 10^9$ ($s^{-1}$) | $k_{nr}$ $\times 10^9$ ($s^{-1}$) |
|---|---|---|---|---|---|---|---|---|---|
| | | | | | $\tau_1$ ($A_1$) | $\tau_2$ ($A_2$) | | | |
| **Toluene** | 366 | 430 | 4067 | 0.011 | 0.51 (78.92) | 1.10 (21.08) | 1.96 | 0.02 | 1.94 |
| **THF** | 367 | 432 | 4100 | 0.054 | | 0.48 (100) | 2.08 | 0.11 | 1.97 |
| **ACN** | 373 | 436 | 3874 | 0.282 | | 4.01 (100) | 0.25 | 0.07 | 0.18 |
| **DMF** | 373 | 437 | 3926 | 0.270 | | 2.96 (100) | 0.34 | 0.09 | 0.25 |
| **PC** | 378 | 447 | 4084 | 0.378 | | 5.05 (100) | 0.19 | 0.07 | 0.12 |
| **MeOH** | 383 | 453 | 4035 | 0.026 | 0.31 (90.82) | 2.09 (9.18) | 3.23 | 0.08 | 3.14 |
| **Water** | 394 | 462 | 3736 | 0.015 | 0.15 (97.99) | 1.30 (2.01) | 6.67 | 0.10 | 6.57 |

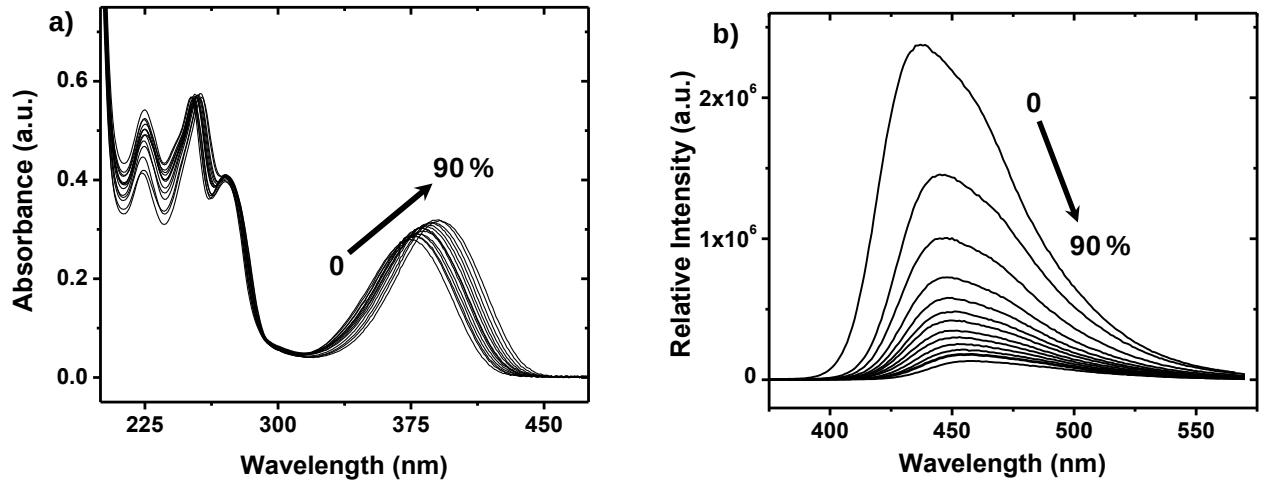


**Figure S3.** Variation in the a) Absorption and b) Emission spectra of **ADDOH** at various percentage of water.

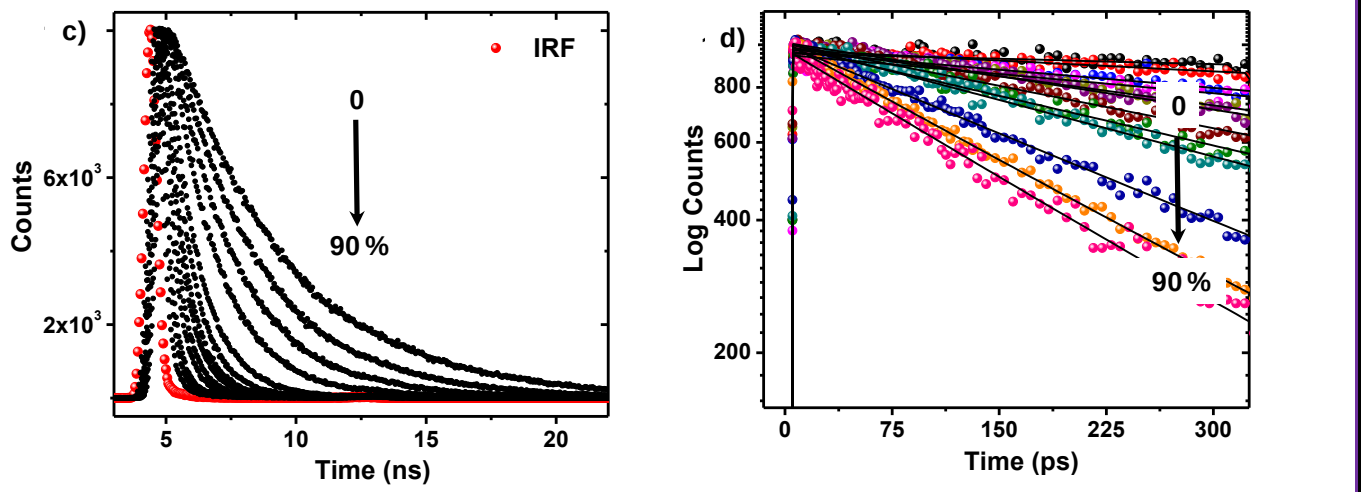


**Figure S4.** Variation in the Fluorescence decay profile of **ADDOH** at various percentage of water measured using a) TCSPC b) Femtosecond upconversion technique.

**Table S3.** Fluorescence lifetime data of **ADDOH** in ACN-Water mixture

| % $H_2O$ | [$H_2O$] M | $\tau_1$ (ns) | $\tau_2$ (ns) | $A_1$ (%) | $A_2$ (%) |
|---|---|---|---|---|---|
| 0 | 0 | 4.11 | - | 100 | - |
| 2.5 | 1.38 | 3.29 | - | 100 | - |
| 5 | 2.78 | 2.50 | - | 100 | - |
| 10 | 5.56 | 1.92 | - | 100 | - |
| 15 | 8.33 | 1.31 | - | 100 | - |
| 20 | 11.11 | 1.03 | - | 100 | - |
| 25 | 13.89 | 0.86 | - | 100 | - |
| 30 | 16.67 | 0.76 | - | 100 | - |
| 40 | 22.22 | 0.59 | - | 100 | - |
| 50 | 27.78 | 0.50 | - | 100 | - |
| 60 | 33.33 | 0.43 | - | 100 | - |
| 70 | 38.88 | 0.30 | 1.10 | 93.66 | 6.34 |
| 80 | 44.44 | 0.25 | 1.11 | 95.12 | 4.88 |
| 90 | 49.99 | 0.21 | 1.61 | 97.43 | 2.57 |

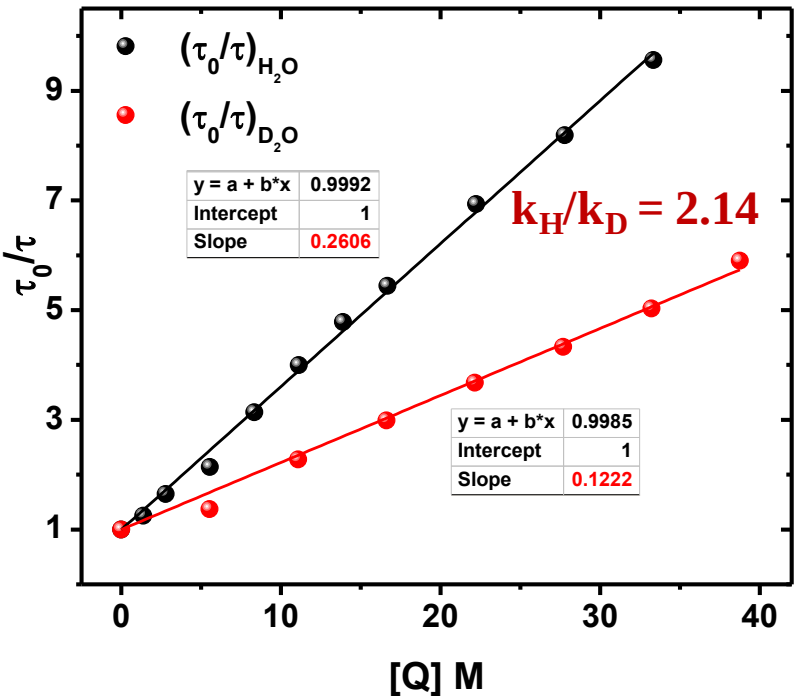


**Figure S5.** S-V plot showing the quenching of **ADDOH** fluorescence lifetime by $H_2O/D_2O$

## Discussion - D1

In case of ADDOH,

$$\Delta G_{PET} = E^0(PhOH/PhOH^{+\cdot}) - E^0(ADD^*/ADD^-)$$

$$E^0(ADD^*/ADD^-) = \{E^0(ADD/ADD^{-\cdot}) + E_{0\text{-}0}\}$$

The excited state reduction potential of acridinedione $E^0(ADD^*/ADD^-)$ is the summation of ground state reduction potential of acridinedione $E^0(ADD/ADD^{-\cdot})$ and the vibrational zero electronic energy of the photo excited ADD unit $E_{0\text{-}0}$ in the respective solvent. Among which the $E_{0\text{-}0}$ value of ADD in ACN (3.02 V) becomes less positive (~120 mV) with the increase in addition of water as shown in the **figure S6a** and thermodynamically opposes the PET process. On the other hand, for the ground state reduction potential of acridinedione, no clear conclusion can be made based on the available experimental data. Ulrich et al., has mentioned that the $E_{redn}^{1/2}$ value of phenyl derivative of ADD as -1.656 V Vs NHE in ACN.[7] But Srividya et al., has done a detail electrochemical studies on basic ADD dyes and declares that there is no reduction

peak corresponding to the direct reduction of the ADD dye is observed in the potential range of 0 to -1.5 V in ACN.[8] Whereas Mohan et al., has determined the reduction potential of the ADD fluorophore in aqueous environment as -0.586 $\pm$ 0.03 V Vs NHE through pulse radiolysis technique.[9] Hence, to resolve the ambiguity in the reduction potential value, we carried out cyclic voltametric studies in both acetonitrile and water. But as what Srividya et al., has stated, we don't find any reduction peak for ADD in the potential range of 0 to -2 V in both the solvents as shown in **figure S6b**. But, for a decade our research group has investigated the excited state behaviour of different ADD derivatives and indubitably established that ADD is a good electron acceptor in the excited state.[10-15] So, to have an account on the influence of protic solvent in altering the excited state reduction potential of the ADD dye the following studies were carried out.

The fluorescence quantum yield ($\phi_f$) and lifetime ($\tau$) value of ADDOH and ADDOMe in acetonitrile is given in **table S4** where the difference in their $\phi_f$ values are due to the difference in the oxidation potential of phenol and methoxy benzene (in acetonitrile $E_{Ox}^{Phenol}$ ~ 1.15 – 1.45 V; $E_{Ox}^{Anisole}$ ~ 1.60 – 1.81 V Vs SCE)[16,17]. In protic solvent, phenol can act as both hydrogen bond donor as well as acceptor but it prefers to be a hydrogen bond donor (because it is relatively more acidic than the protic solvent) which significantly shifts the oxidation potential of phenol to a less positive value. But methoxy benzene can behave only as hydrogen bond acceptor which in turn decreases its tendency to undergo oxidation and it is expected to shift its oxidation potential to a more positive value. If there is not much variation in the excited state reduction potential of the ADD unit in protic and aprotic solvent, then the fluorescence quantum yield and lifetime value of ADDOMe is expected to be high in protic solvents and less in case of ADDOH. To our dismay, the values are less in ADDOMe and very less in ADDOH as shown in the **figure S7** and **table S4**. These observations clearly implicate that the excited state reduction potential of ADD is significantly reduced in the protic solvents and shift towards more positive value which in turn facilitate the intramolecular PET process. It is further supplemented by the discussion D2.

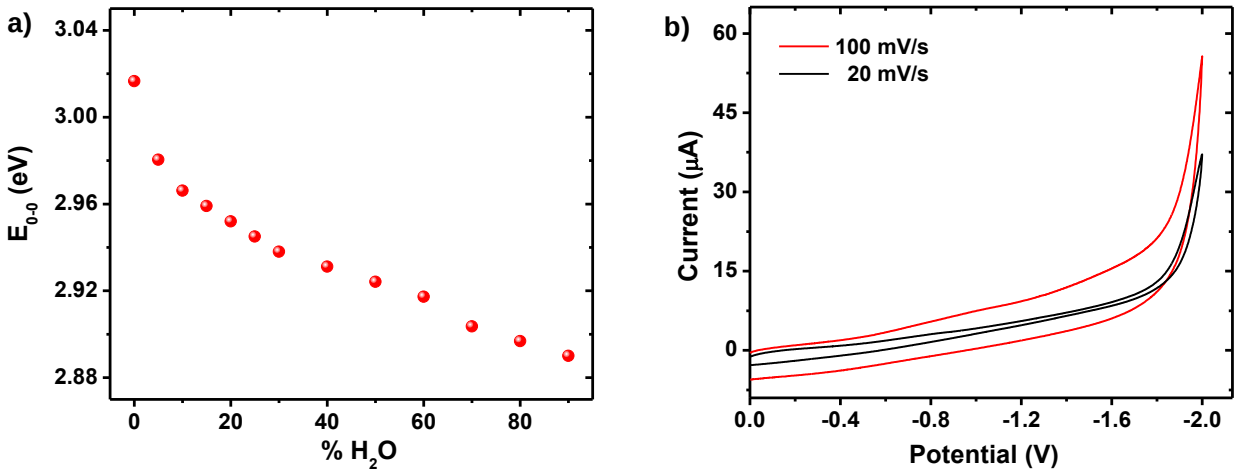


**Figure S6.** a) Variation in the $E_{0-0}$ vlaue of **ADD** with the increasing % of water b) Cyclic Voltammogram of **ADD** at different scan rate in ACN.

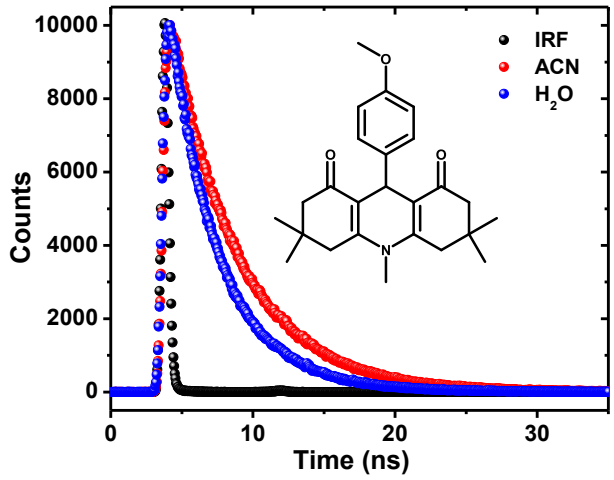


**Figure S7**. Fluorescence decay profile of **ADDOMe** in ACN and Water.

| Solvent | ADDOH | | ADDOMe | |
|---|---|---|---|---|
| | $\phi_f$ | $\tau_f$ (ns) | $\phi_f$ | $\tau_f$ (ns) |
| ACN | 0.282 | 4.22 | 0.312 | 4.67 |
| $H_2O$ | 0.015 | 0.15 | 0.258 | 3.62 |

**Table S4**. Fluorescence Quantum yield and lifetime value of **ADDOH** and **ADDOMe** in ACN and Water

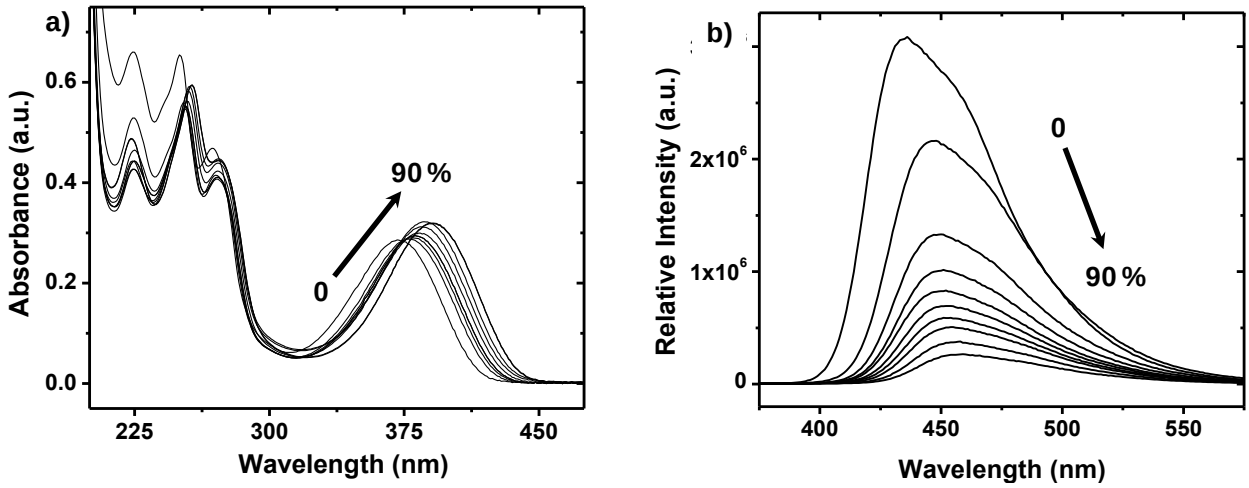


**Figure S8.** Variation in the a) Absorption and b) Emission spectra of **ADDOH** at various percentage of $D_2O$.

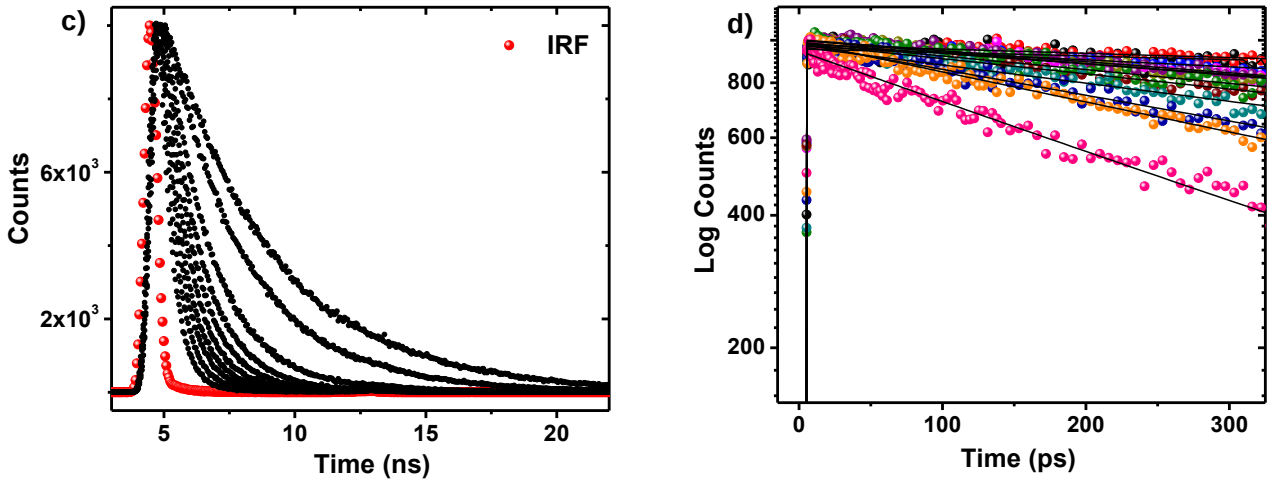


**Figure S9.** Variation in the Fluorescence decay profile of **ADDOH** at various percentage of $D_2O$ measured using a) TCSPC b) Femtosecond upconversion technique.

**Table S5.** Fluorescence lifetime data of **ADDOH** in ACN-$D_2O$ mixture

| % $H_2O$ | [$D_2O$] M | $\tau_1$ (ns) | $\tau_2$ (ns) | $A_1$ (%) | $A_2$ (%) |
|---|---|---|---|---|---|
| 0 | 0 | 4.12 | - | 100 | - |
| 10 | 5.54 | 3.01 | - | 100 | - |
| 20 | 11.07 | 1.81 | - | 100 | - |
| 30 | 16.61 | 1.38 | - | 100 | - |
| 40 | 22.14 | 1.12 | - | 100 | - |
| 50 | 27.68 | 0.95 | - | 100 | - |
| 60 | 33.22 | 0.82 | - | 100 | - |
| 70 | 38.75 | 0.70 | - | 100 | - |
| 80 | 44.29 | 0.55 | 1.74 | 95.62 | 4.38 |
| 90 | 49.82 | 0.44 | 1.61 | 96.85 | 3.15 |

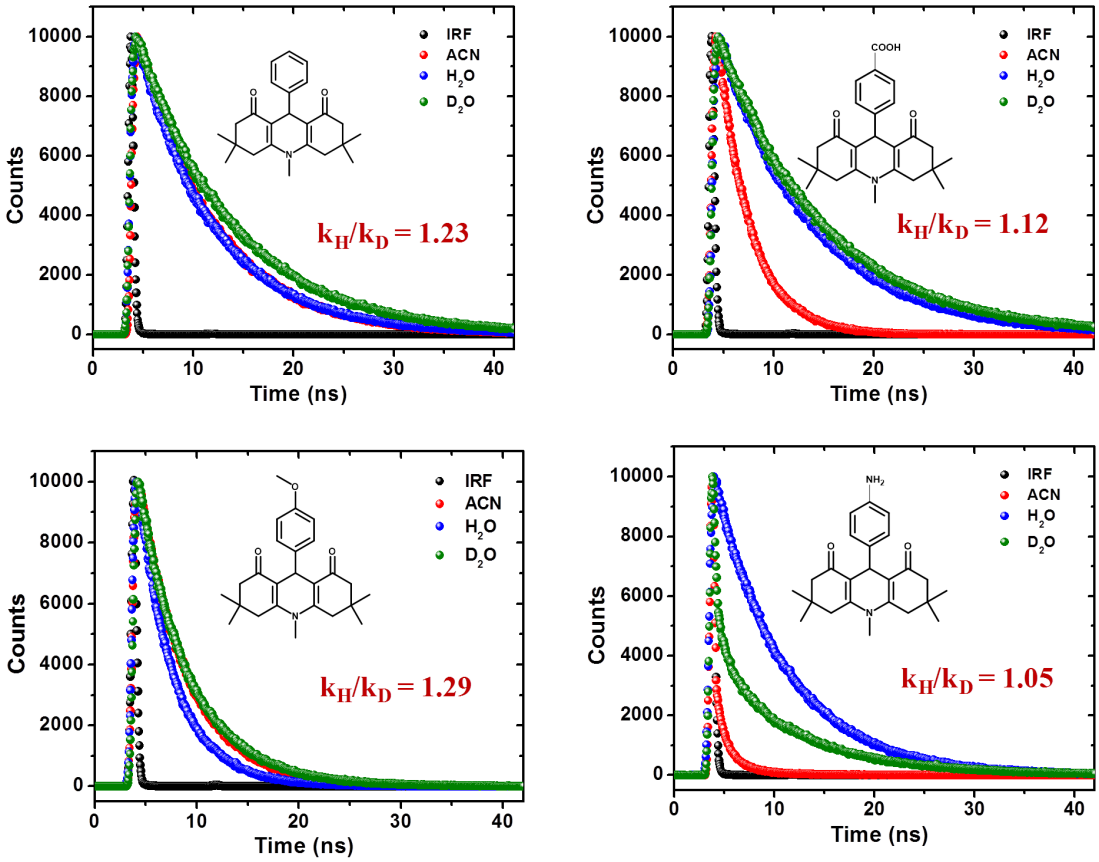


**Figure S10.** Kinetic isotopic influence on fluorescence rate constant for different **ADD** derivatives.

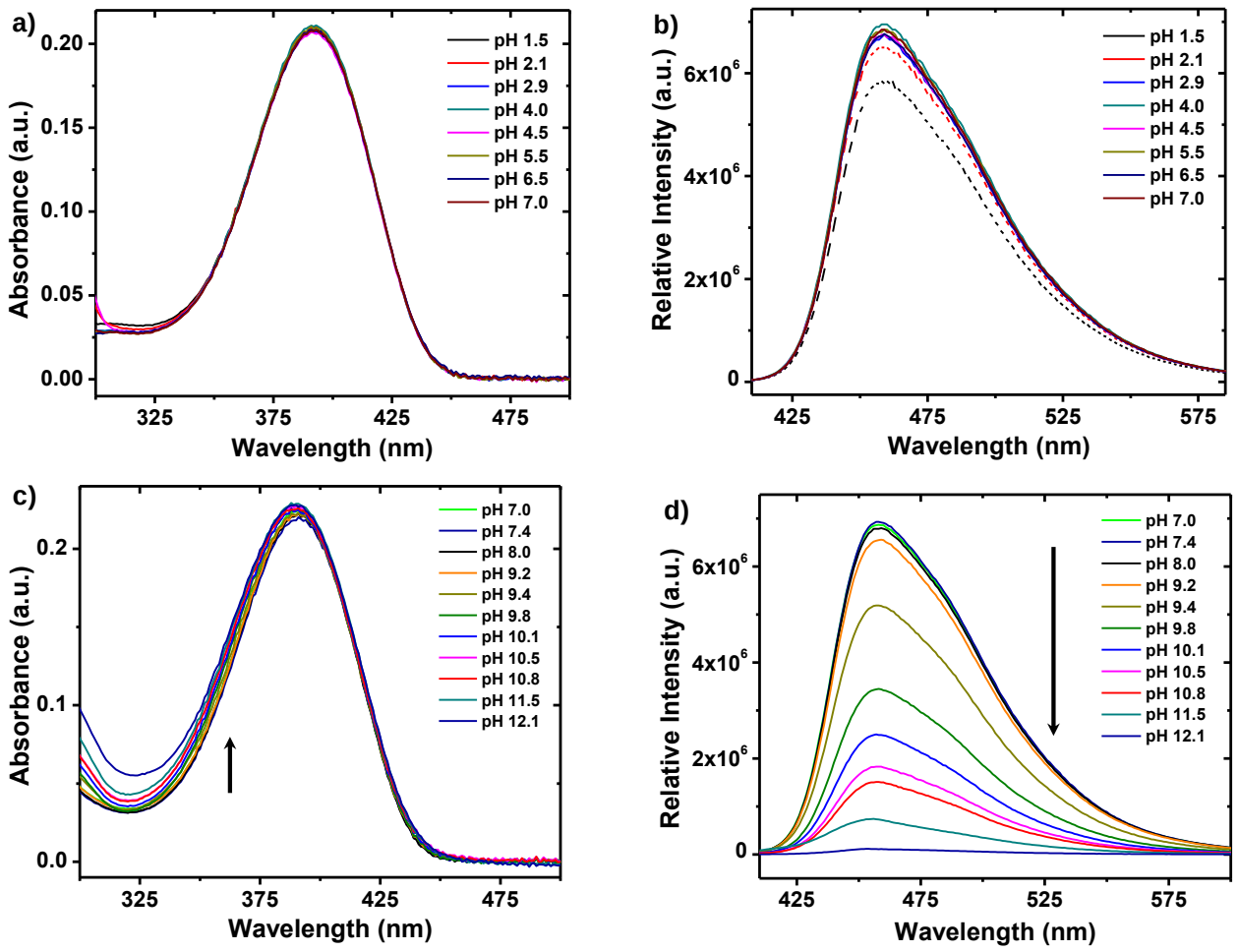


**Figure S11.** Variation in the absorption and emission spectra of **ADDOH** at different pH.

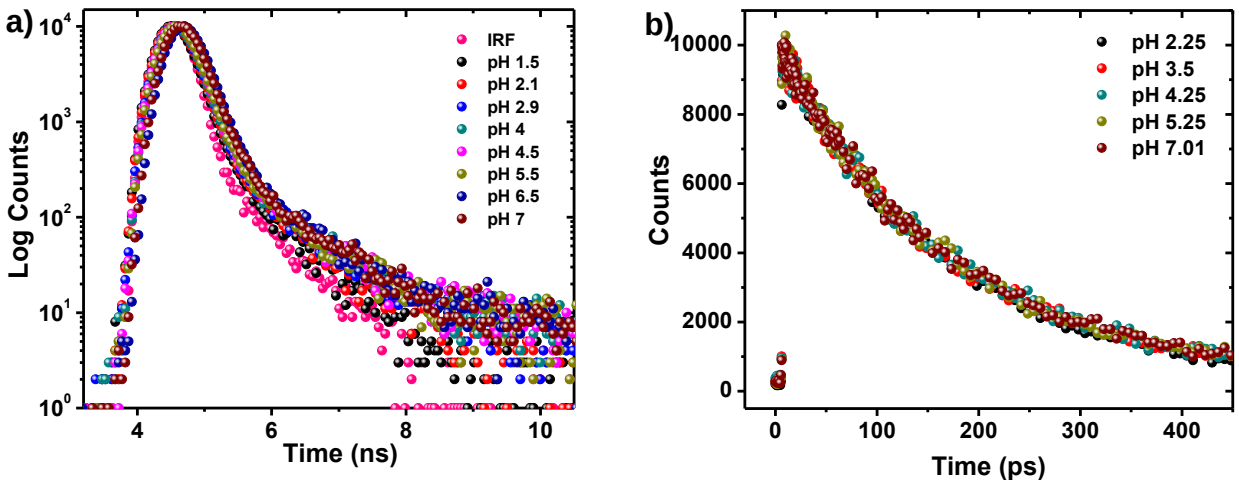


**Figure S12.** Variation in the Fluorescence decay profile of **ADDOH** in acidic region recorded using a) TCSPC b) Femtosecond upconversion technique.

**Table S6.** Fluorescence lifetime value of **ADDOH** in acidic region measured using TCSPC and femtosecond upconversion technique.

| pH | $\tau_1$ (ns) | $\tau_2$ (ns) | $A_1$ (%) | $A_2$ (%) |
|---|---|---|---|---|
| 1.50 | 0.137 | - | 100 | - |
| 2.05 | 0.144 | 1.24 | 98.43 | 1.57 |
| 2.90 | 0.150 | 1.66 | 98.09 | 1.91 |
| 4.00 | 0.150 | 1.62 | 97.70 | 2.30 |
| 4.50 | 0.150 | 1.72 | 98.00 | 2.00 |
| 5.50 | 0.141 | 1.45 | 97.88 | 2.12 |
| 6.50 | 0.152 | 1.30 | 97.99 | 2.01 |
| 7.01 | 0.160 | 1.62 | 98.25 | 1.75 |

| pH | $\tau_1$ (ns) | $A_1$ (%) |
|---|---|---|
| 2.25 | 0.166 | 100 |
| 3.50 | 0.167 | 100 |
| 4.25 | 0.170 | 100 |
| 5.25 | 0.173 | 100 |
| 7.04 | 0.171 | 100 |

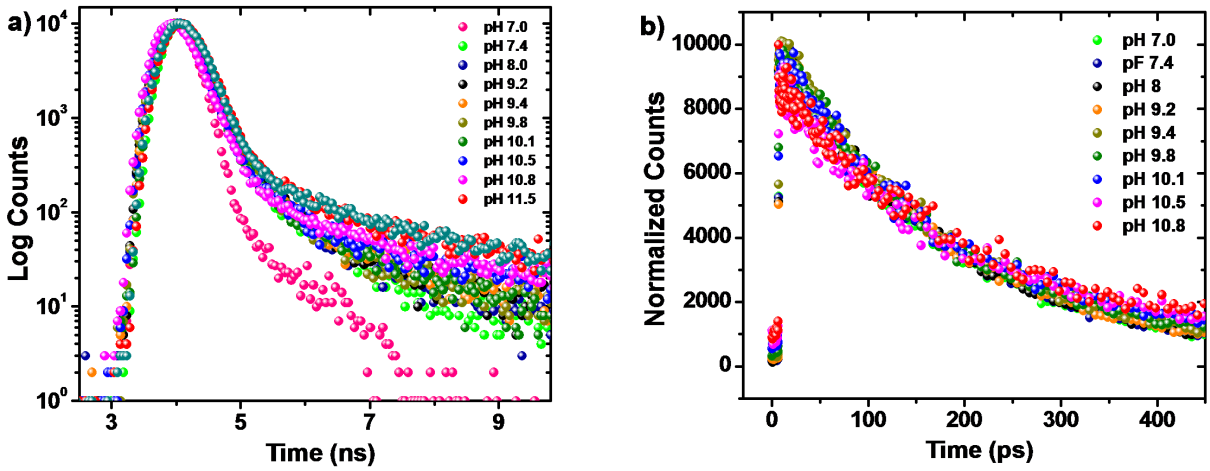


**Figure S13.** Variation in the Fluorescence decay profile of **ADDOH** in basic regime recorded using a) TCSPC at) b) Femtosecond upconversion technique.

**Table S7.** Fluorescence lifetime value of **ADDOH** in basic regime measured using TCSPC and femtosecond upconversion technique.

| pH | $\tau_1$ (ns) | $\tau_2$ (ns) | $A_1$ (%) | $A_2$ (%) |
|---|---|---|---|---|
| 7.01 | 0.160 | 1.62 | 98.25 | 1.75 |
| 7.4 | 0.174 | 1.13 | 95.78 | 4.22 |
| 8 | 0.183 | 1.22 | 95.72 | 4.28 |
| 9.2 | 0.178 | 1.59 | 96.29 | 3.71 |
| 9.4 | 0.177 | 1.39 | 96.76 | 3.54 |
| 9.8 | 0.174 | 1.99 | 97.10 | 2.10 |
| 10.1 | 0.181 | 2.17 | 96.16 | 3.84 |
| 10.5 | 0.184 | 2.46 | 95.59 | 4.41 |
| 10.8 | 0.191 | 2.49 | 93.11 | 6.89 |
| 11.5 | 0.182 | 2.47 | 92.89 | 7.11 |

| pH | $\tau_1$ (ns) | $A_1$ (%) |
|---|---|---|
| 7.04 | 0.171 | 100 |
| 7.4 | 0.179 | 100 |
| 8.4 | 0.176 | 100 |
| 9.2 | 0.176 | 100 |
| 9.4 | 0.175 | 100 |
| 9.8 | 0.180 | 100 |
| 10.1 | 0.184 | 100 |
| 10.5 | 0.182 | 100 |
| 10.8 | 0.190 | 100 |
| 11.1 | 0.188 | 100 |
| 11.4 | 0.193 | 100 |

# Discussion -D2

Fluorescence lifetime value of ADDOH in ACN was quenched with the increase in addition percentage of water. In this case, the variation in the oxidation potential of the phenol as a function of water percentage is only ~300 mV. Whereas on varying the pH (2 - 10) of the solution of ADDOH in water, the variation in the oxidation potential of the phenol was ~ 450 mV (based on its Pourbaix diagram) but it doesn't quenches the fluorescence lifetime. It clearly indicates that the reduction potential of the acridinedione was relatively more negative (difficult to reduce) in the polar aprotic solvent like acetonitrile (as it was stated in **discussion D1**) and it becomes less negative (and so easy to reduce) in the aqueous environment. Hence, on adding water to the solution of ADDOH in ACN, the free energy associated with the electron transfer process becomes more negative, which in turn quenches its fluorescence lifetime drastically. Whereas on varying the pH between 2 - 12, there is not much change in the reduction potential of the ADD fluorophore but it is already less negative and hence easy to reduce in aqueous environment. So, tuning only the oxidation potential of the phenol as a function of pH have no impact on quenching the fluorescence lifetime.

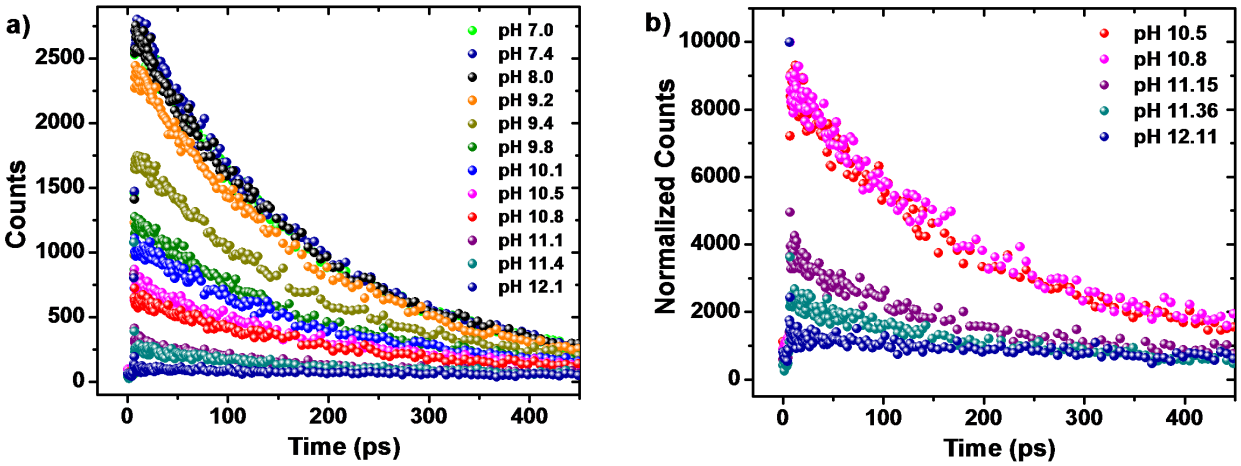


**Figure S14.** a) Fluorescence decay profile of **ADDOH** in picosecond time domain showing the decrease in intensity with the increase in pH. b) Due to low fluorescence quantum yield, the fluorescence decay profile at high pH is dominated by the Raman scattering

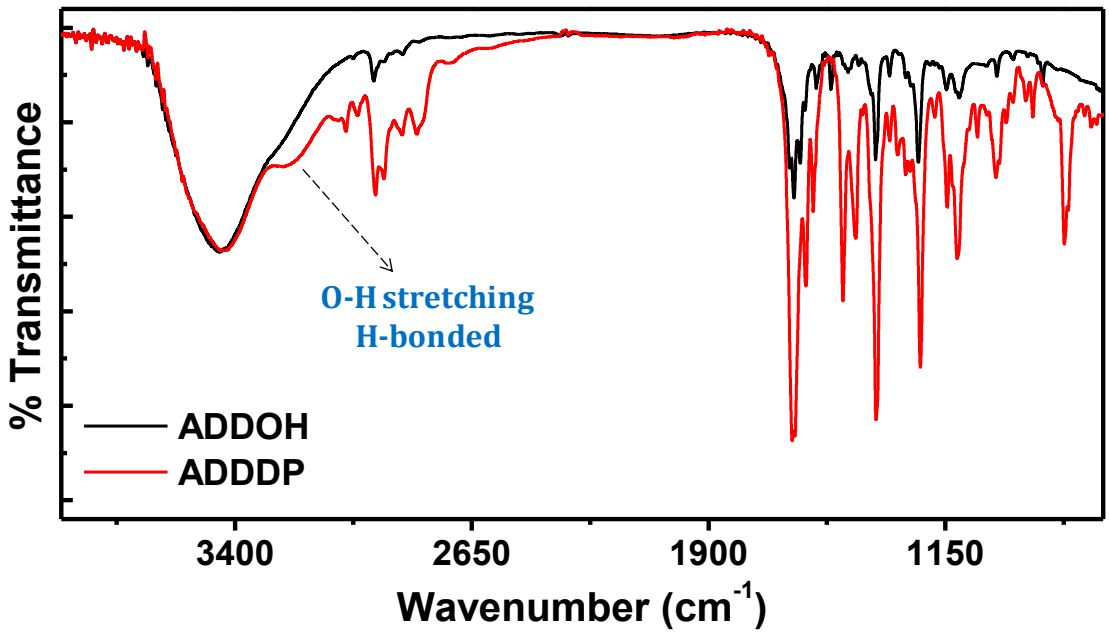


**Figure S15.** IR spectrum of **ADDOH** and **ADDDP** (in KBr) showing the presence of intramolecular hydrogen bond in **ADDDP.**

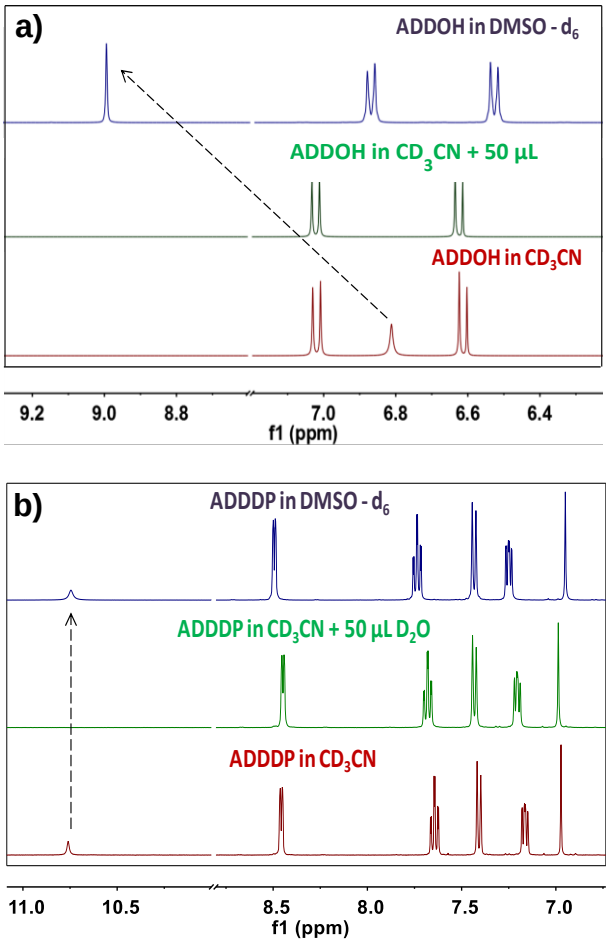


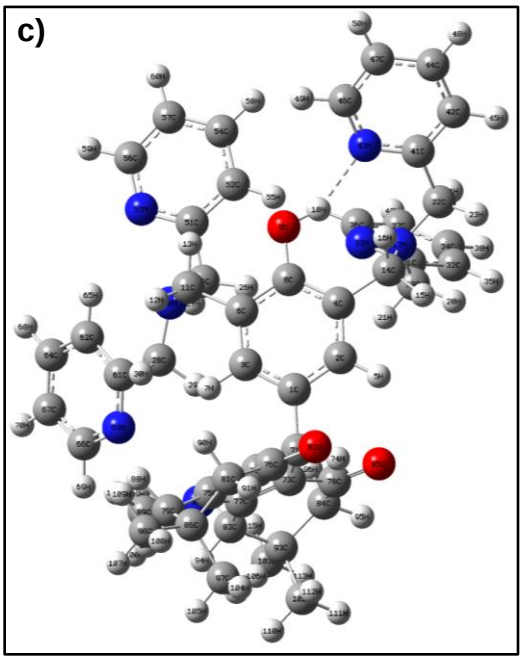


**Figure S16.** $^{1}$H NMR spectrum of **a) ADDOH** and **b) ADDDP** in different deuterated solvents. **c)** The optimized ground state geometry of ADDDP was determined using DFT calculations (Gaussian 09.C.01 version).

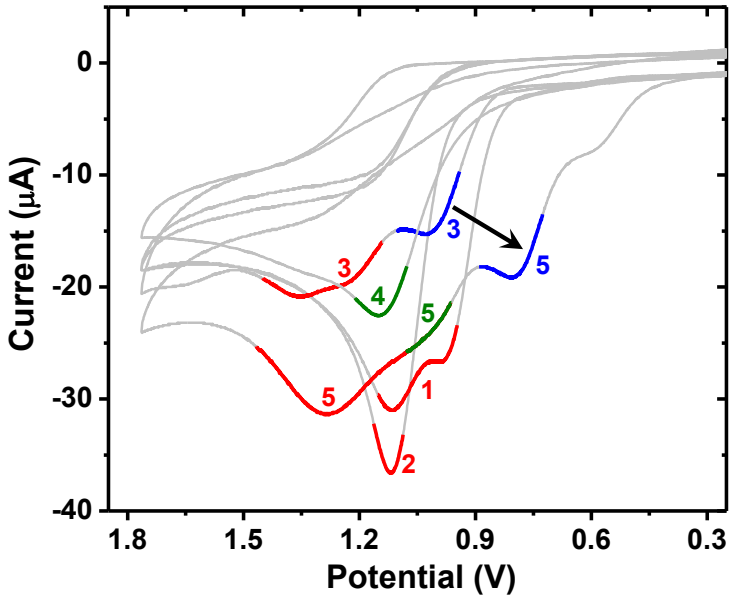


**Figure S17.** Cyclic Voltammogram of 1) **ADD0** 2) **ADD1** 3) **ADDOH** 4) **DPA** 5) **ADDDP** measured at a scan rate of 100 mV/s using Ag/Agcl as reference electrode in ACN. The arrow represents the shift in the oxidation potential of the phenol after DPA substitution.

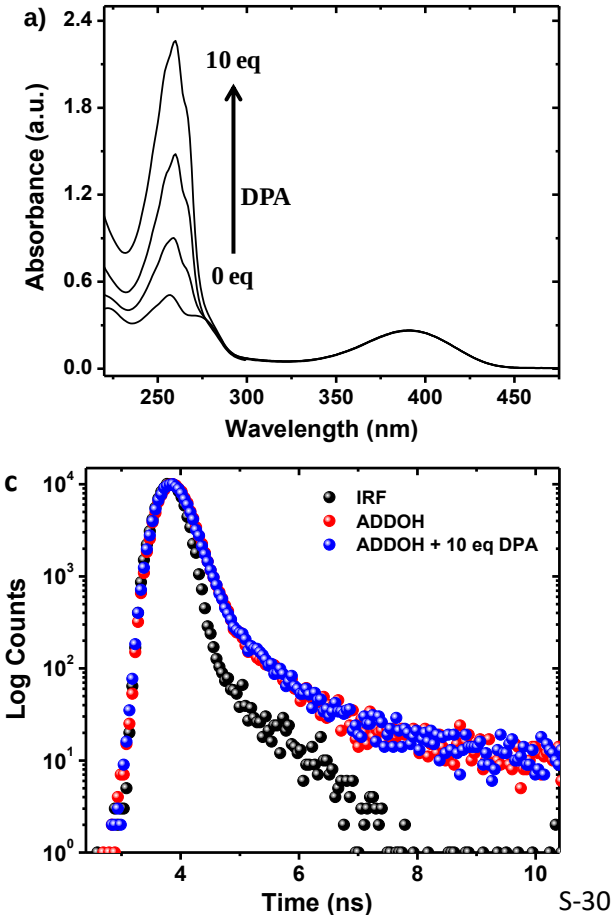


**Figure S18.** Variation in the a) Absorption Spectra b) Emission Spectra c) Fluorescence decay profile of ADDOH with the addition of 0 -10 equivalents of DPA.

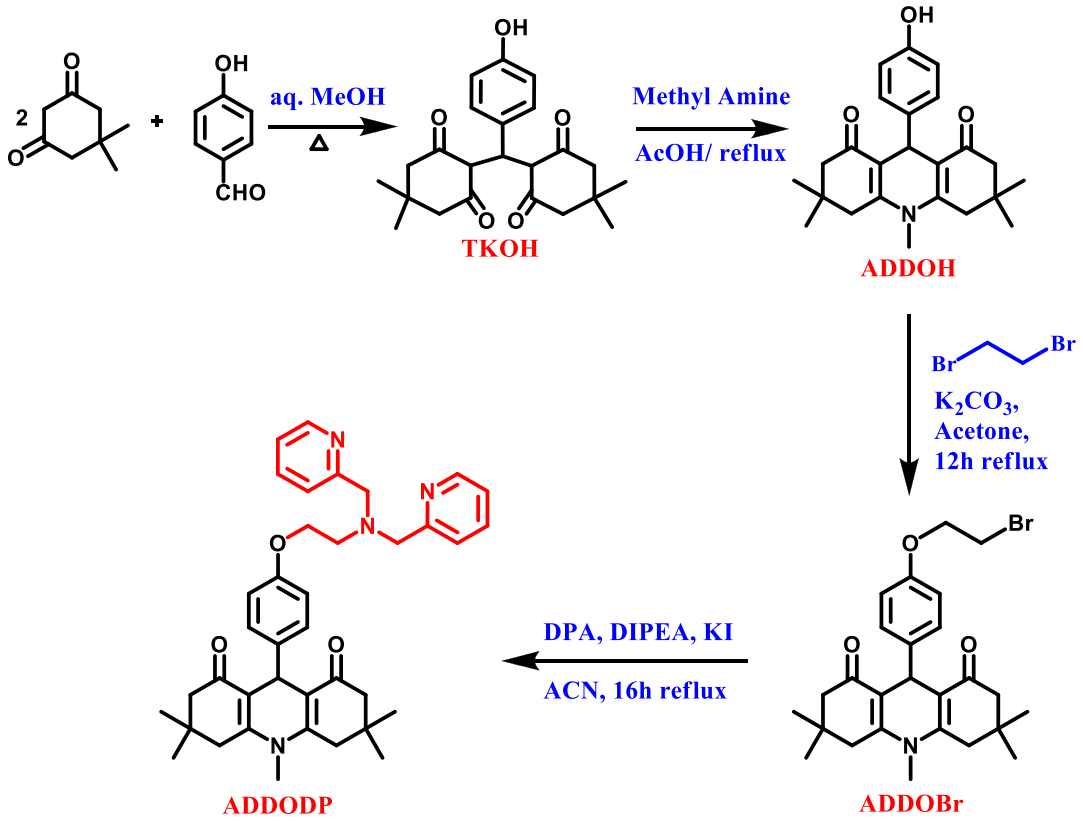


**Scheme S2.** Synthetic scheme for **ADDODP**

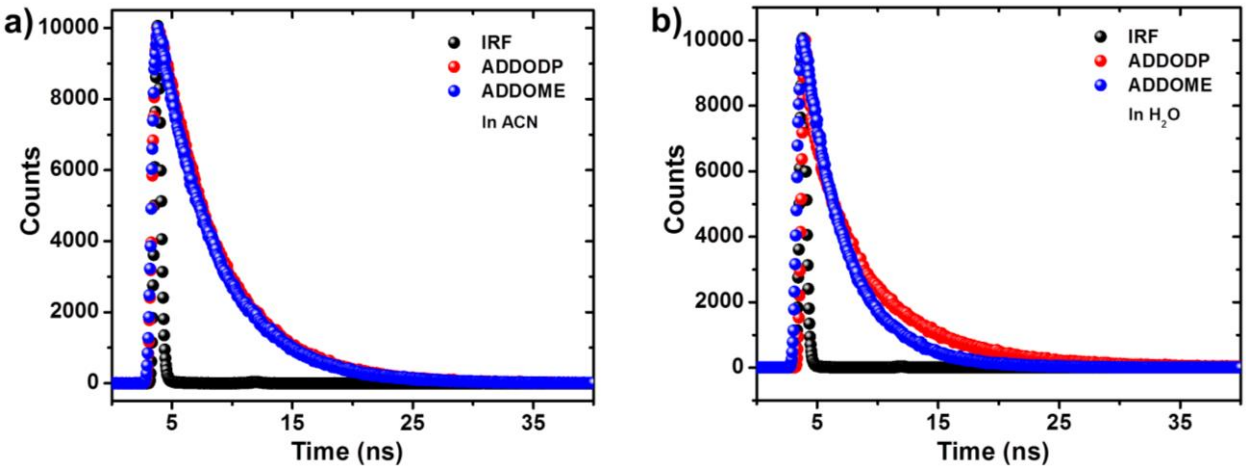


**Figure S19.** Fluorescence decay profile of **ADDODP** and **ADDOMe** a) In ACN b) In $H_2O$.

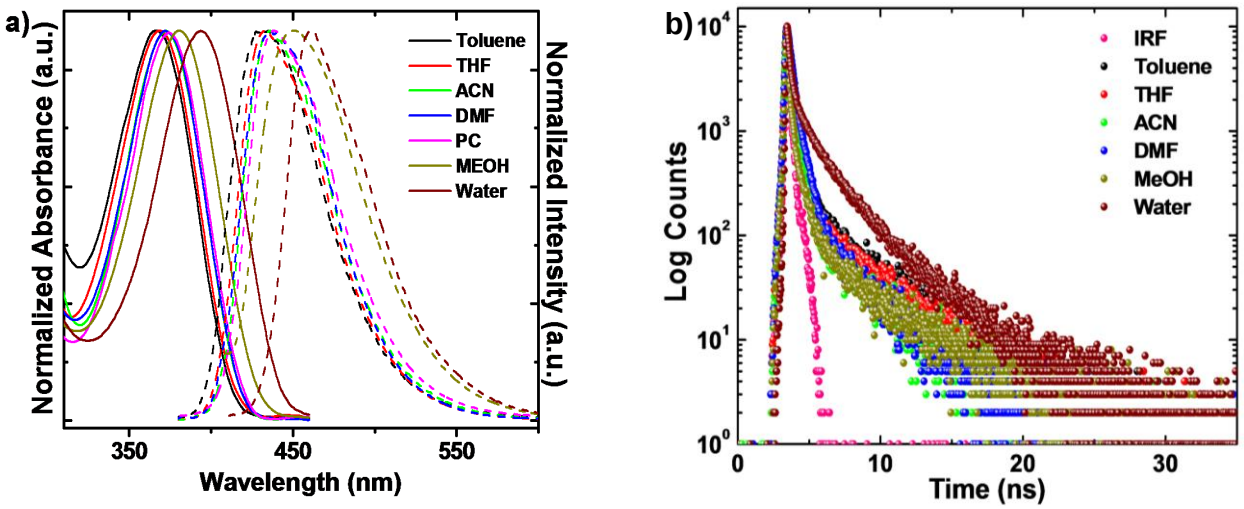


**Figure S20.** a) Absorption and emission spectra of **ADDDP** in different solvents b) Fluorescence decay profile of ADDDP in different solvents.

**Table S8.** Photophysical data of **ADDDP** in different solvents

| Solvent | Abs ($\lambda_{max}$) nm | $\varepsilon$ ($M^{-1}$ $cm^{-1}$) | Emi ($\lambda_{max}$) nm | Stokes Shift ($cm^{-1}$) | $\phi_f$ |
|---|---|---|---|---|---|
| Tol | 366 | 5416 | 436 | 4386 | 0.011 |
| THF | 369 | 5520 | 437 | 4217 | 0.012 |
| ACN | 373 | 5675 | 439 | 4030 | 0.018 |
| DMF | 372 | 7467 | 441 | 4206 | 0.014 |
| PC | 374 | 7632 | 442 | 4114 | 0.016 |
| MeOH | 380 | 6811 | 451 | 4143 | 0.003 |
| Water | 394 | 8665 | 460 | 3642 | 0.002 |

**Table S9.** Fluorescence lifetime data of **ADDDP** in different solvents measured using TCSPC.

| Solvent | $\tau_1$ (ps) | $\tau_m$ (ns) | $\tau_2$ (ns) | $A_1$ (%) | $A_m$ (%) | $A_2$ (%) | k x $10^{10}$ ($s^{-1}$) | | |
|---|---|---|---|---|---|---|---|---|---|
| | | | | | | | $k_{total}$ | $k_f$ | $k_{nr}$ |
| Toluene | 186 | | 2.96 | 92.38 | | 7.62 | 0.53 | 0.006 | 0.53 |
| THF | 130 | | 2.86 | 85.58 | | 14.42 | 0.81 | 0.009 | 0.80 |
| ACN | 176 | | 2.92 | 87.11 | | 12.89 | 0.87 | 0.016 | 0.85 |
| DMF | 229 | | 2.07 | 88.65 | | 11.35 | 0.44 | 0.006 | 0.43 |
| PC | 370 | | 4.56 | 65.82 | | 34.18 | 0.43 | 0.007 | 0.42 |
| MeOH | 85 | | 2.72 | 87.08 | | 12.92 | 6.67 | 0.002 | 6.65 |
| Water | 79 | 1.06 | 3.18 | 58.85 | 27.80 | 13.35 | 12.50 | 0.003 | 12.48 |

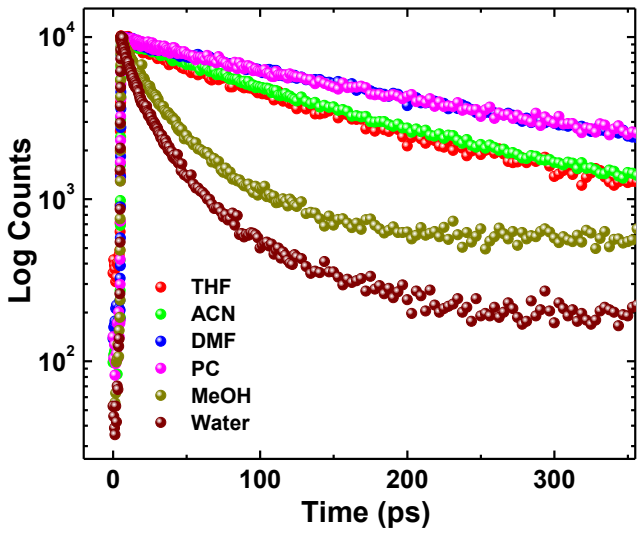


**Figure S21.** Fluorescence decay profile of **ADDDP** in different solvents measured using femtosecond upconversion technique.

| Solvent | $\tau_u$ (ps) | $\tau_1$ (ps) | $A_u$ (%) | $A_1$ (%) |
|---|---|---|---|---|
| THF | | 123 | | 100 |
| ACN | | 113 | | 100 |
| DMF | | 228 | | 100 |
| PC | | 232 | | 100 |
| MeOH | 15 | 41 | 42 | 52 |
| Water | 4.5 | 33 | 45 | 53 |

**Table S10.** Fluorescence lifetime value of **ADDDP** in different solvents measured using femtosecond upconversion technique.

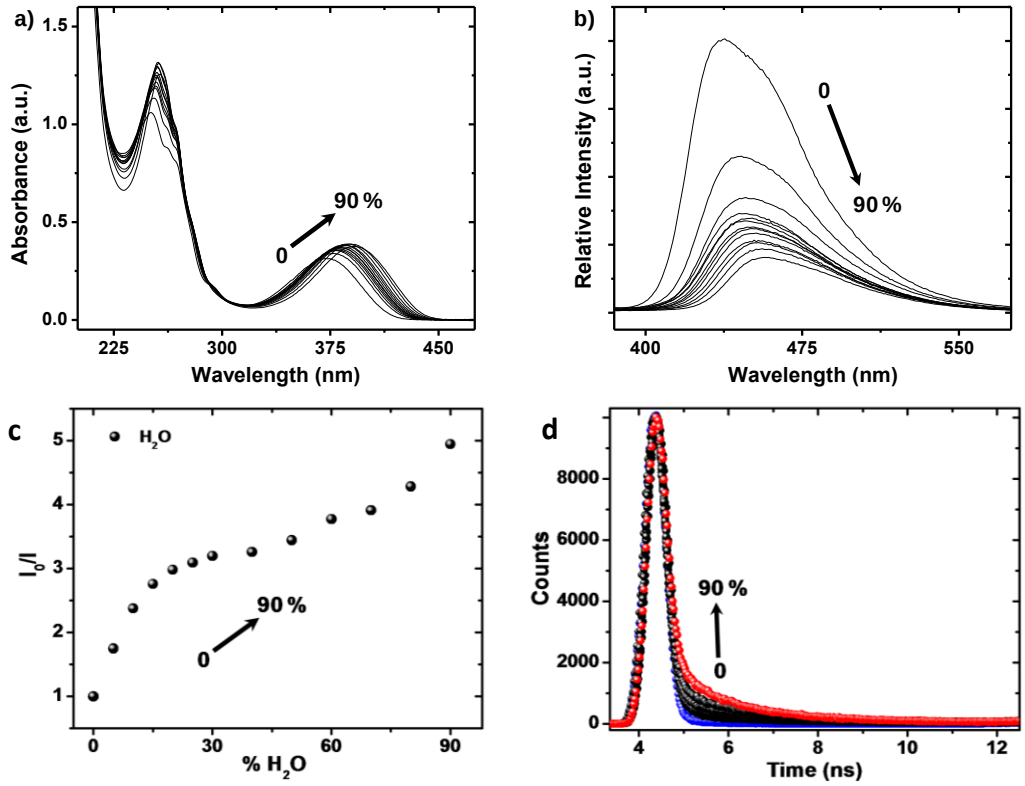


**Figure S22**. Variation in the a) Absorption b) Emission spectra c) S-V plot showing the non-linear quenching of emission intensity. d) Fluorescence decay profile of **ADDDP** in acetonitrile with the increase in addition % of water.

**Table S11.** Fluorescence lifetime value of **ADDDP** in ACN with the increase in addition percentage of water measured using TCSPC.

| % $H_2O$ | $\tau_1$ (ns) | $\tau_m$ (ns) | $\tau_2$ (ns) | $A_1$ (%) | $A_m$ (%) | $A_2$ (%) |
|---|---|---|---|---|---|---|
| 0 | 0.180 | | 3.01 | 85.29 | | 14.71 |
| 5 | 0.122 | | 3.47 | 86.39 | | 13.61 |
| 10 | 0.115 | | 3.29 | 83.43 | | 16.57 |
| 20 | 0.112 | | 3.59 | 83.87 | | 16.13 |
| 30 | 0.115 | | 3.69 | 83.90 | | 16.10 |
| 40 | 0.113 | | 3.57 | 82.37 | | 17.63 |
| 50 | 0.119 | | 3.70 | 80.81 | | 19.19 |
| 60 | 0.036 | 0.610 | 3.87 | 74.85 | 6.65 | 18.50 |
| 70 | 0.036 | 0.826 | 3.74 | 70.76 | 9.77 | 19.47 |
| 80 | 0.036 | 1.012 | 3.76 | 62.84 | 16.41 | 20.75 |
| 90 | 0.036 | 1.080 | 3.52 | 55.07 | 26.32 | 18.61 |

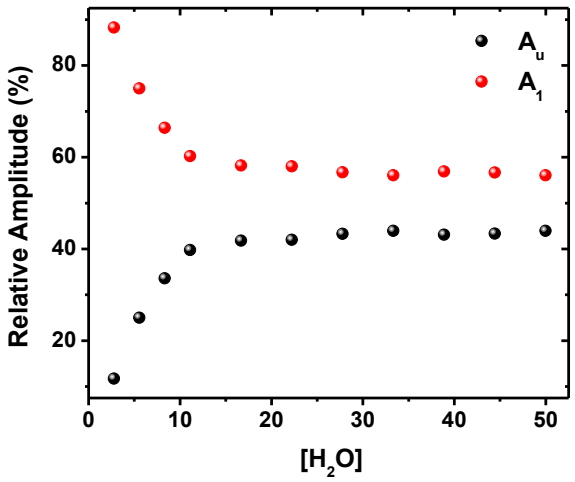


**Figure S23.** Variation in the relative amplitude of the shorter components of **ADDDP** with the increase in addition percentage of water.

**Table S12.** Fluorescence lifetime value of **ADDDP** in ACN with the increase in addition percentage of water.

| % $H_2O$ | [$H_2O$] M | $\tau_u$ (ps) | $\tau_1$ (ps) | $A_u$ (%) | $A_1$ (%) |
|---|---|---|---|---|---|
| 0 | 0 | | 111.12 | | 100.00 |
| 5 | 2.78 | 15.11 | 81.05 | 11.74 | 88.26 |
| 10 | 5.56 | 15.10 | 81.01 | 25.02 | 74.98 |
| 15 | 8.33 | 15.02 | 80.50 | 33.58 | 66.42 |
| 20 | 11.11 | 14.82 | 80.20 | 39.75 | 60.25 |
| 30 | 16.67 | 13.13 | 76.35 | 41.81 | 58.19 |
| 40 | 22.22 | 12.09 | 69.07 | 42.00 | 58.00 |
| 50 | 27.78 | 9.98 | 61.80 | 43.31 | 56.69 |
| 60 | 33.33 | 9.41 | 56.03 | 43.93 | 56.07 |
| 70 | 38.88 | 8.10 | 46.01 | 43.10 | 56.90 |
| 80 | 44.44 | 6.74 | 41.32 | 43.36 | 56.64 |
| 90 | 49.99 | 4.80 | 34.39 | 43.93 | 56.07 |

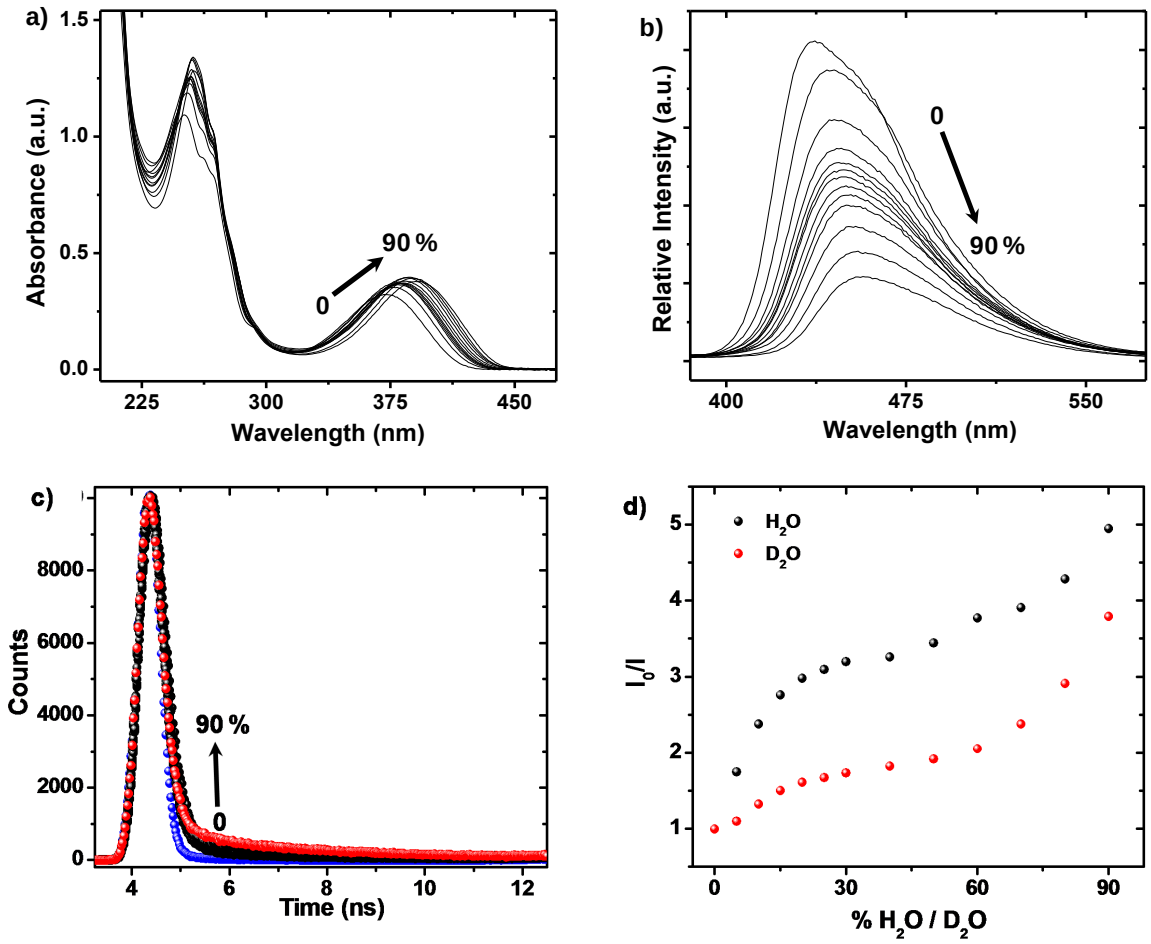


**Figure S24**. Variation in the a) Absorption b) Emission spectra **($\lambda_{ex}$ = 300 nm)** c) Fluorescence decay profile of **ADDDP** in acetonitrile with the increase in addition % of $D_2O$ ($\lambda_{ex}$ = **375 nm** and monitored at**)** d) S-V plot showing the non-linear quenching of emission intensity.

**Table S13.** Fluorescence lifetime value of **ADDDP** in ACN with the increase in addition percentage of $D_2O$ measured using TCSPC.

| % $D_2O$ | $\tau_1$ (ns) | $\tau_2$ (ns) | $A_1$ (%) | $A_2$ (%) |
|---|---|---|---|---|
| 0 | 0.180 | 3.04 | 85.89 | 14.11 |
| 5 | 0.175 | 4.08 | 90.03 | 9.97 |
| 10 | 0.156 | 4.47 | 87.21 | 12.79 |
| 20 | 0.151 | 4.34 | 86.15 | 13.85 |
| 30 | 0.148 | 4.59 | 84.56 | 15.44 |
| 40 | 0.155 | 4.87 | 84.34 | 15.66 |
| 50 | 0.155 | 4.71 | 82.78 | 17.22 |
| 60 | 0.152 | 4.44 | 83.32 | 16.68 |
| 70 | 0.152 | 4.27 | 80.71 | 19.29 |
| 80 | 0.148 | 3.91 | 75.68 | 24.32 |
| 90 | 0.149 | 3.47 | 69.83 | 30.17 |

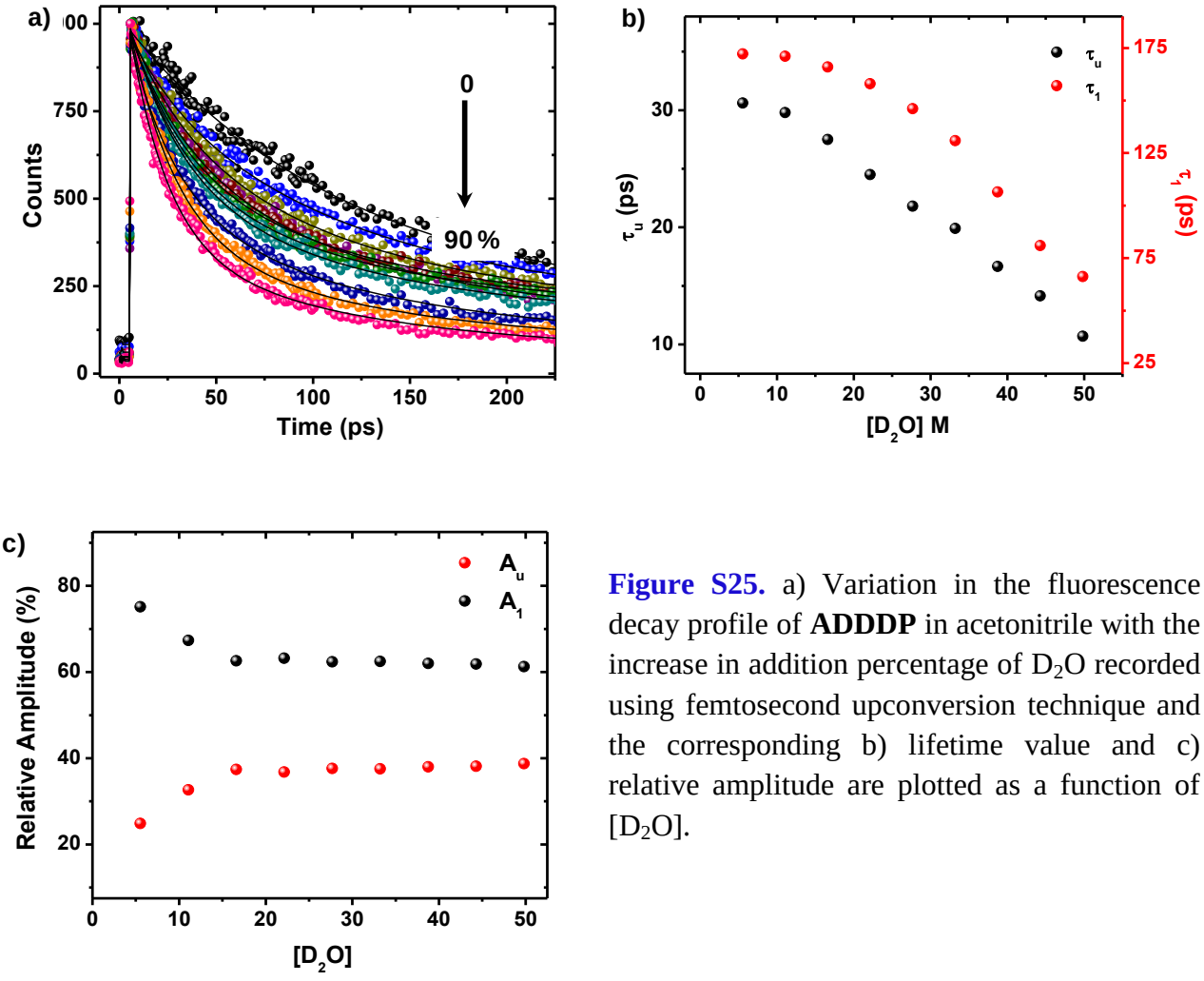


**Figure S25.** a) Variation in the fluorescence decay profile of **ADDDP** in acetonitrile with the increase in addition percentage of $D_2O$ recorded using femtosecond upconversion technique and the corresponding b) lifetime value and c) relative amplitude are plotted as a function of $[D_2O]$.

**Table S14.** Fluorescence lifetime value of **ADDDP** in ACN with the increase in addition percentage of $D_2O$ measured using femto upconversion.

| % $D_2O$ | [$D_2O$] | $\tau_u$ (ps) | $\tau_1$ (ps) | $A_u$ (%) | $A_1$ (%) |
|---|---|---|---|---|---|
| 0 | 0 | | 111.12 | | 100.00 |
| 10 | 5.56 | 30.6 | 172.2 | 24.85 | 75.15 |
| 20 | 11.11 | 29.8 | 171.1 | 32.66 | 67.34 |
| 30 | 16.67 | 27.5 | 166 | 37.38 | 62.62 |
| 40 | 22.22 | 24.5 | 158 | 36.78 | 63.22 |
| 50 | 27.78 | 21.8 | 146.15 | 37.62 | 62.38 |
| 60 | 33.33 | 19.9 | 130.87 | 37.53 | 62.47 |
| 70 | 38.88 | 16.65 | 106.46 | 37.98 | 62.02 |
| 80 | 44.44 | 14.15 | 81.01 | 38.16 | 61.84 |
| 90 | 49.99 | 10.7 | 66.22 | 38.72 | 61.28 |

## Discussion - D3

The fluorescence quantum yield of ADDDP in acetonitrile is 1.8 %, which is very much (15.5 times) lesser than that of ADDOH in ACN due to the efficient intramolecular hydrogen bonding interaction. The strength of this intramolecular hydrogen bond can be evaluated using $pK_a$ slider rule, i.e., lower the $\Delta pK_a$ value (difference in the $pK_a$ value of the hydrogen bond donor and acceptor) then stronger the hydrogen bond.[18] In this case, the $pK_a$ value of the phenol (hydrogen bond donor) in acetonitrile[19] is 29.14, and for DPA (the hydrogen bond acceptor) the pKa value in acetonitrile is unavailable. Hence, the $pK_a$ value of analogous TEA[20] was taken as 18.82 and the $\Delta pK_a$ value is determined to be ~10, so hydrogen bond with medium strength. Even such a moderate interaction in acetonitrile significantly quenches the fluorescence quantum yield and lifetime of acridinedione fluorophore by effectively involving in the MSEPT process. Applying the similar approach for ADDOH in water ($\Delta pK_a$ = $pK_a$ (PhOH) - $pK_a$ ($H_3O^+$)) yields the same result (~10) and the extent of fluorescence quenching is also similar to that of ADDDP in ACN. It shows that, ortho substituting the amine (2 equivalents) for a unimolecular MSEPT process in acetonitrile is analogous to exposing the unsubstituted phenol to the very large excess

of water for a bimolecular MSEPT process. Also that, the variation in the oxidation potential of the unsubstituted phenol in acetonitrile with the increase in addition percentage of water is due to the continuous variation in the $\Delta pK_a$ value i.e., the hydrogen bond strength. So, the stronger the hydrogen bond more effective will be the MSEPT process.

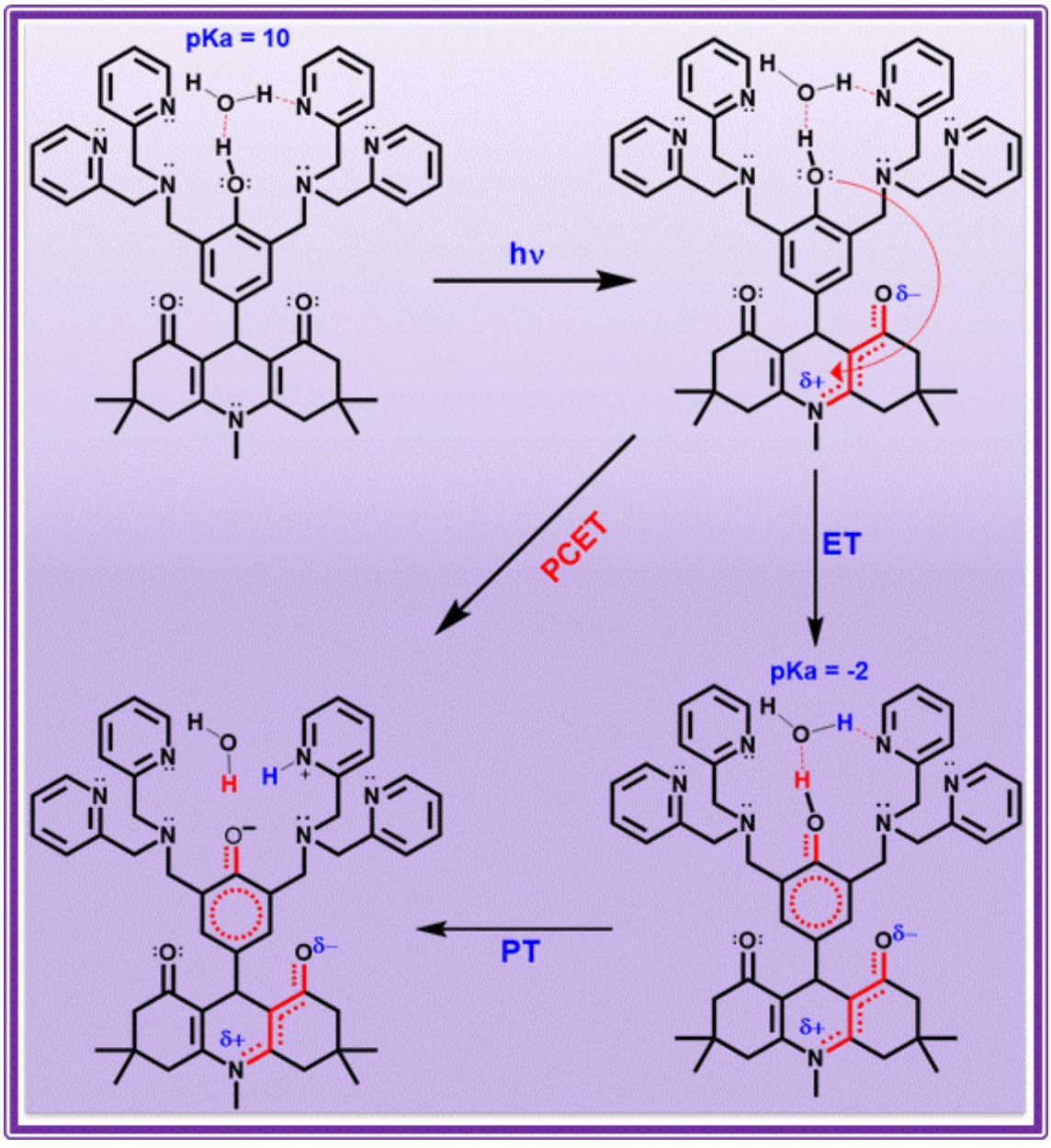


**Scheme S3.** Light driven water mediated PCET process in ADDDP.

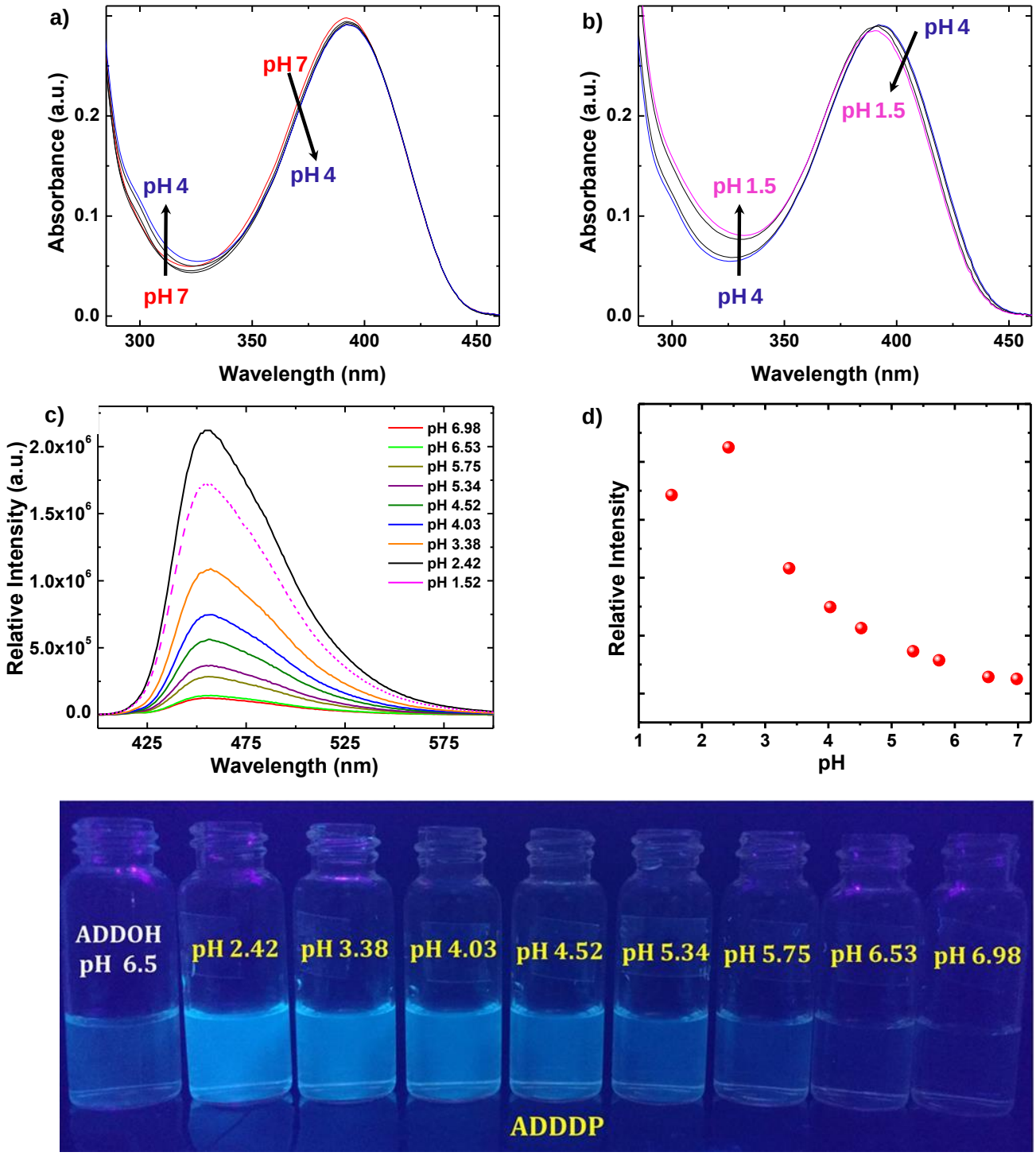


**Figure S26.** Variation in the a) & b) Absorption c) Emission spectra d) Emission intensity of ADDDP as a function of pH e) **ADDDP** solutions in different pH under UV lamp.

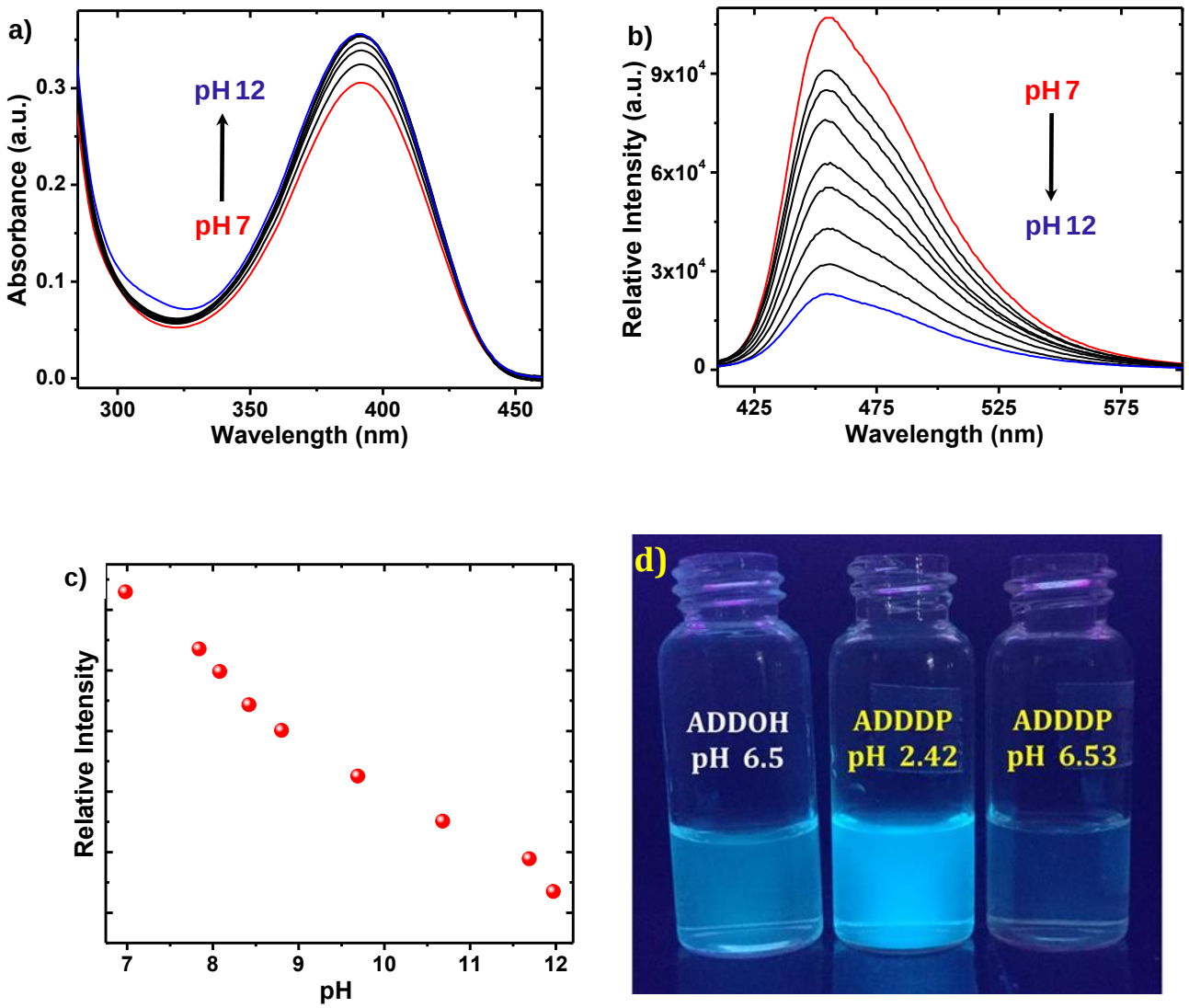


**Figure S27.** Variation in the a) Absorption b) Emission spectra c) Emission intensity of ADDDP as a function of pH d) **ADDDP** and **ADDOH** solutions in different pH under UV lamp.

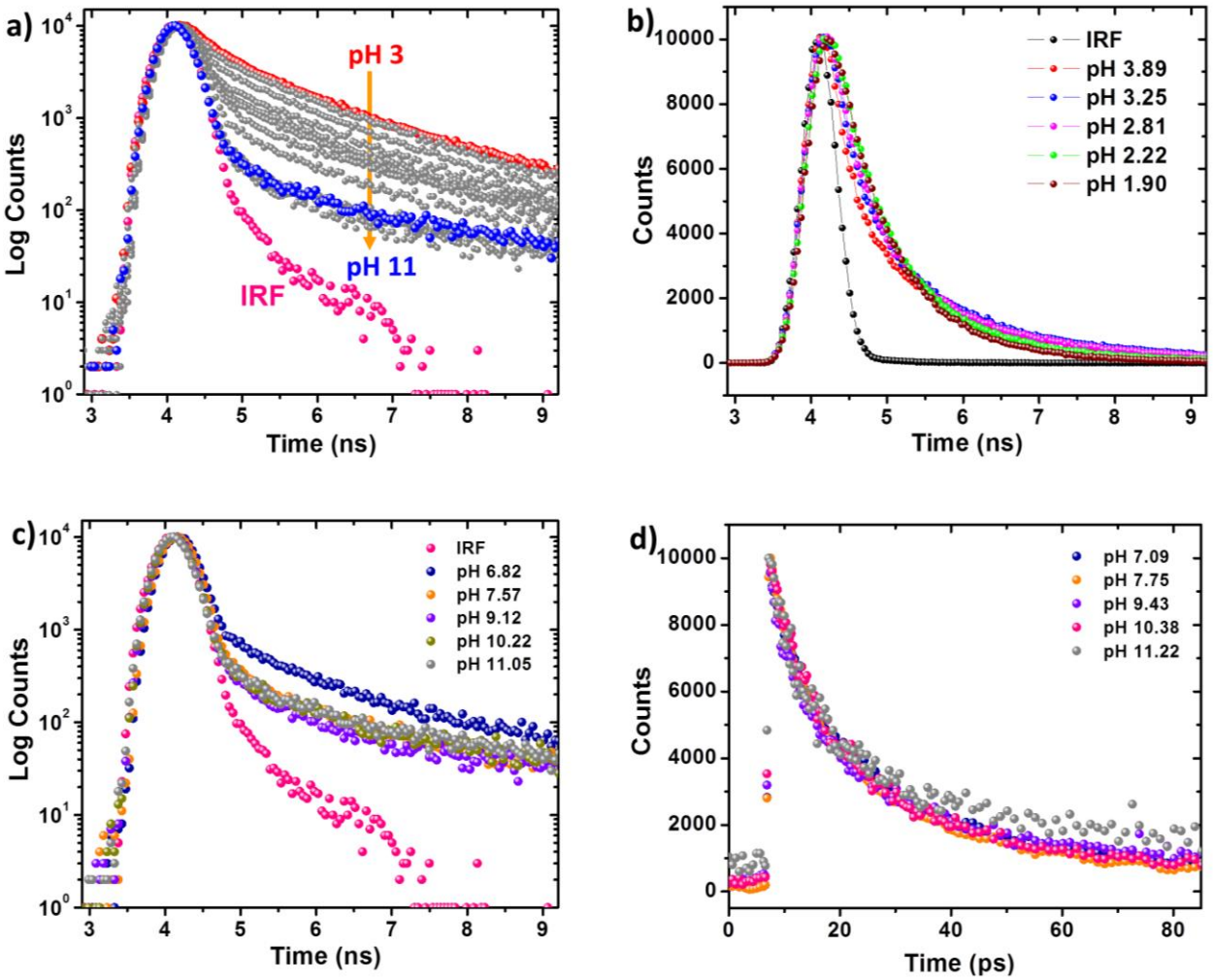


**Figure S28.** a) Fluorescence decay profile of **ADDDP** as a function of pH b) Fluorescence decay profile showing the proton induced fluorescence quenching of longer decay component and simultaneous increase in the lifetime of ultrashort component in the acidic condition. No change in the Fluorescence decay profile in basic condition measured using c) TCSPC d) Femtosecond upconversion technique.

**Table S15.** Fluorescence lifetime value of **ADDDP** at different pH measured using TCSPC.

| pH | $\tau_1$ (ps) | $\tau_m$ (ns) | $\tau_2$ (ns) | $A_1$ (%) | $A_m$ (%) | $A_2$ (%) |
|---|---|---|---|---|---|---|
| 1.50 | | 0.534 | 0.980 | | 70.82 | 29.18 |
| 1.90 | | 0.608 | 1.30 | | 71.42 | 28.58 |
| 2.22 | 0.043 | 0.640 | 1.56 | 17.54 | 52.79 | 29.67 |
| 2.81 | 0.054 | 0.824 | 2.60 | 25.04 | 46.85 | 28.10 |
| 3.25 | 0.051 | 0.913 | 2.66 | 26.07 | 45.48 | 28.45 |
| 3.89 | 0.061 | 0.987 | 2.69 | 28.44 | 45.32 | 26.25 |
| 4.67 | 0.089 | 1.03 | 2.86 | 35.54 | 43.48 | 20.98 |
| 5.14 | 0.091 | 1.08 | 2.96 | 46.37 | 37.38 | 16.25 |
| 5.51 | 0.072 | 1.08 | 3.02 | 54.98 | 30.91 | 14.11 |
| 5.79 | 0.079 | 1.03 | 3.12 | 58.63 | 27.79 | 13.57 |
| 6.82 | 0.070 | 1.07 | 3.65 | 75.47 | 12.97 | 11.56 |
| 7.57 | 0.065 | 1.03 | 4.01 | 88.40 | 5.10 | 6.49 |
| 9.12 | 0.053 | 1.03 | 4.02 | 91.54 | 3.16 | 5.30 |
| 10.22 | 0.063 | 1.02 | 4.01 | 88.41 | 4.03 | 7.55 |
| 11.05 | 0.057 | 1.03 | 4.01 | 87.93 | 4.24 | 7.83 |

**Figure S29.** On decreasing the pH, evolution of $\tau_m$ and $\tau_2$ with the consumption of $\tau_1$, was shown by plotting the relative amplitude of $A_1$ and sum of $A_m$ and $A_2$ as a function of pH.

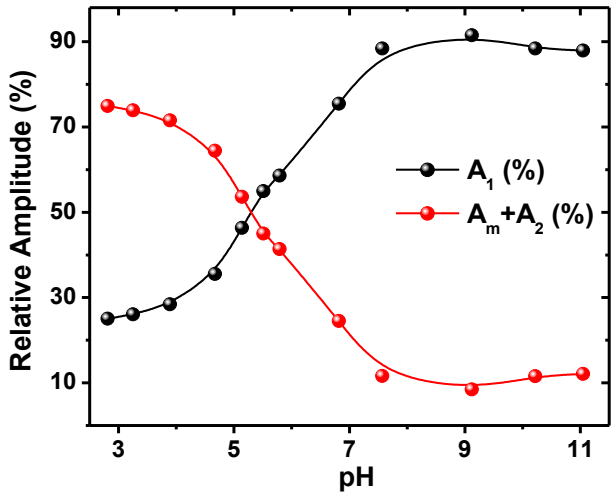


**Table S16**. Fluorescence lifetime value of **ADDDP** at different pH measured using femto upconversion technique.

| pH | $\tau_u$ (ps) | $\tau_1$ (ps) | $\tau_m$ (ns) | $A_u$ (%) | $A_1$ (%) | $A_m$ (%) |
|---|---|---|---|---|---|---|
| 2.04 | | | 0.53 | | | 100 |
| 2.37 | | 175.21 | 0.64 | | 17.33 | 82.67 |
| 2.69 | 15.80 | 175.02 | 0.80 | 5.15 | 28.51 | 66.34 |
| 2.93 | 15.13 | 123.78 | 0.83 | 19.18 | 28.31 | 52.51 |
| 3.15 | 14.20 | 106.50 | 0.90 | 22.15 | 34.77 | 43.08 |
| 3.46 | 12.65 | 92.38 | 0.95 | 26.93 | 40.90 | 32.17 |
| 3.85 | 11.65 | 68.45 | 0.98 | 34.33 | 41.39 | 24.28 |
| 4.11 | 10.71 | 62.39 | 1.00 | 37.58 | 43.71 | 18.71 |
| 4.70 | 9.86 | 50.34 | 1.00 | 35.45 | 51.25 | 13.30 |
| 5.22 | 8.53 | 43.42 | 1.00 | 39.50 | 53.17 | 7.33 |
| 6.17 | 7.55 | 38.82 | 1.00 | 44.31 | 52.69 | 3.00 |
| 7.10 | 6.92 | 30.39 | 1.00 | 49.20 | 49.06 | 1.74 |
| 9.43 | 6.70 | 28.72 | 1.00 | 52.30 | 42.54 | 5.16 |
| 10.38 | 6.50 | 27.76 | 1.00 | 52.07 | 46.80 | 1.13 |

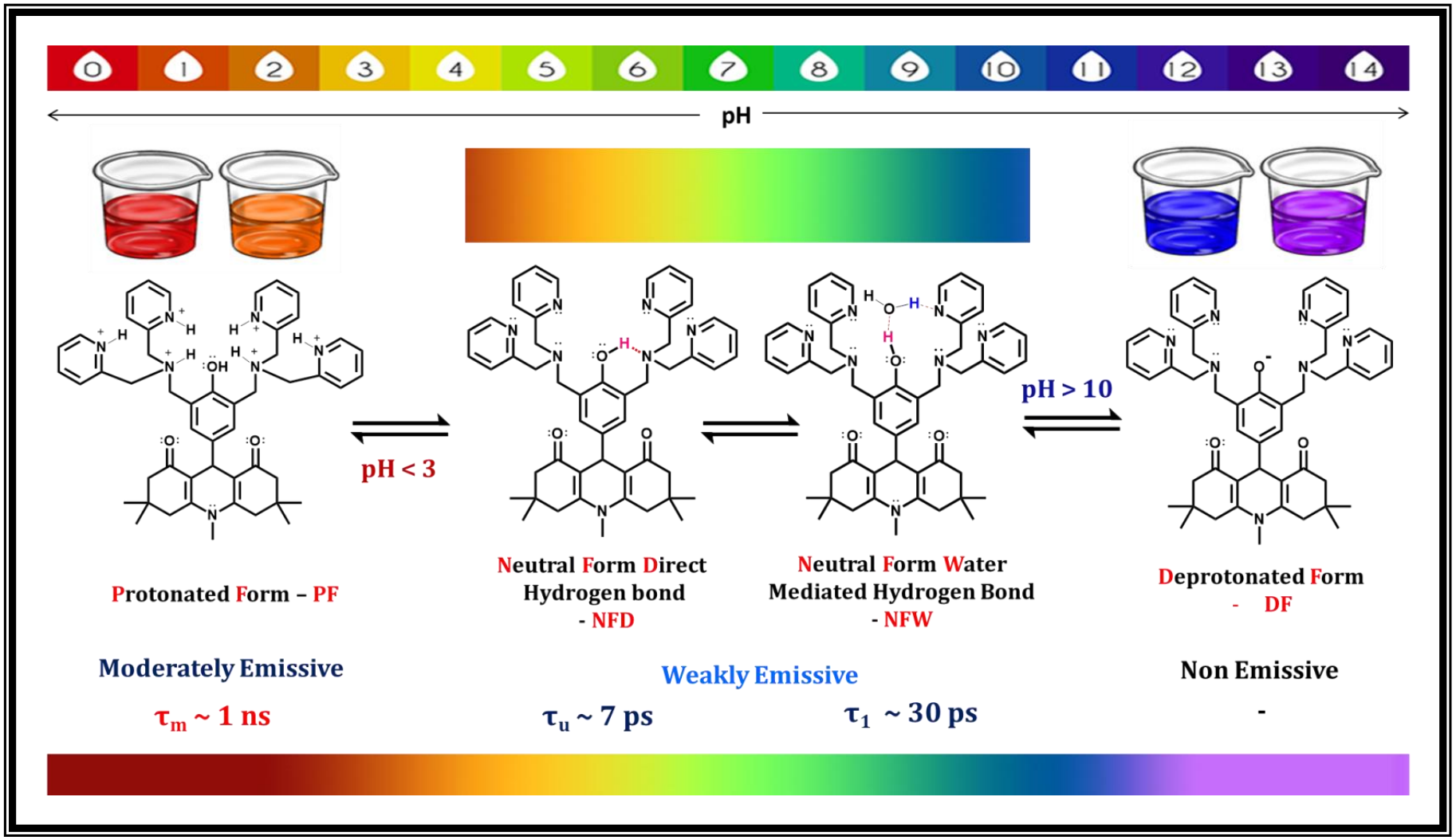


**Figure S30.** Equilibrium between various ground state forms of ADDDP at different pH.

# Discussion - D4

**Time Resolved Absorption Spectrum of ADD derivatives:**

Femtosecond transient absorption spectra were recorded to validate the product resulting from the ultrafast MSEPT process. The UV-Vis absorption spectral behaviour of the products formed due to 'one electron reduction and oxidation' of the acridinediones are well known because of the extensive investigation (and successive publications) by our research group[21-28] using pulse radiolysis and laser flash photolysis techniques. Hence, the transients formed due to the excited state reactions of ADD can be readily identified based on their spectral and kinetic behaviour. However, for better understanding, time resolved absorption spectral studies were carried out for all three ADD derivatives ADD1, ADDOH, ADDDP in both ACN and 1:1 ACN/$H_2O$ mixture.

Absorption spectrum of ADD1 recorded at 100 ps after photoexcitation (figure S31) has shown a strong absorption band at ~440 nm and a broad band with the maximum at ~620 nm in both ACN and 1:1 ACN/$H_2O$ mixture. The positive band at ~620 nm is due to the triplet-triplet absorption of the ADD moiety[24,27,28], whereas the 440 nm band is observed to be due to the transients resulting from photoionization of ADD unit. Photoionization of acridinedione forms radical cation and a solvated electron.[24] This solvated electron further reacts with ADD and forms the anion radical[22-24,28] at a bimolecular rate constant of 1.5 x $10^{10}$ $M^{-1}$ $s^{-1}$. It is both the cation and anion radical of ADD absorb at ~450 nm, however it is already reported that the OD of anion radical is relatively very high and overshadows completely the absorption due to cation radical.[28] The continuous growth of transient decay recorded at 440 nm strongly indicates that the absorption at ~440 nm is primarily due to the anion radical of acridinedione unit.

Time resolved absorption spectrum of ADDOH in ACN has shown analogous behaviour and it is given in figure S32. But in the presence of water, ADDOH is prone to undergo MSEPT process after photoexcitation (Scheme 1). It quenches its excited state drastically and expected to results in the formation of phenoxyl radical cation and anion radical of acridinedione. The femtosecond transient absorption spectrum of ADDOH in 1:1 ACN/$H_2O$ mixture at different time scale and the corresponding transient decay monitored at 440 nm are shown in figure S33. The 440 nm band grows at a relatively faster time scale of ~26 ps and it decays exponentially within 1.5 ns and exhibits a lifetime of ~510 ps. Whereas, the radical anion formed out of

photoionization lives longer, upto few microseconds. Hence, relatively faster 'formation and decay kinetics' of the 440 nm band clearly indicates that the absorption of the anion radical of ADD moiety arises due to the MSEPT process and not because of simple photoionization. Essentially, the efficiency of photoionization is negligible for ADDOH in the presence of water because of the rapid decay of the excited state due to MSEPT process. The other photoproduct, phenoxyl radical cation is expected to absorb at ~410 nm[29] but it might merges with the absorption band of the anion radical of ADD unit.

The transient absorption spectrum of ADDDP in ACN has shown two distinct positive bands at ~410 and 445 nm corresponding to the phenoxyl radical cation and ADD radical anion respectively (figure S34). Formation (30 ps) and decay (150 ps) kinetics of both these bands are alike and much faster than the ADDOH in ACN/$H_2O$ mixture. Thus both these band must emerge from the completely intramolecular MSEPT process exhibited by ADDDP in ACN. In presence of water, the 410 nm band merges with the 440 nm band analogous to ADDOH in ACN/$H_2O$ mixture and it is shown in figure S35. The transient decay of ADDDP monitored at 440 nm has shown a rise time of ~ 1.2 ps and it exhibits a lifetime of ~35 ps in ACN/$H_2O$ mixture. Table S16 compares the formation and decay kinetics of the transient formed due to MSEPT process in ADDOH & ADDDP. Thus, using femtosecond transient absorption spectral studies, the transient formed due to the MSEPT process from ADDOH and ADDDP has been validated.

**Table S16.** Transient lifetimes (rise time and decay time) of ADDOH and ADDDP in ACN, ACN/Water mixture.

| Sample | $\lambda_{abs}$ (nm) | Monitored at 450 nm | |
|---|---|---|---|
| | | Rise Time $\tau_1$ (ps) | Decay Time $\tau_2$ (ps) |
| ADDOH (In ACN/Water mixture) | 440 | 26 | 510 |
| ADDDP (In ACN) | 410, 440 | 30 | 150 |
| ADDDP (In ACN/Water mixture) | 440 | 1.2 | 35 |

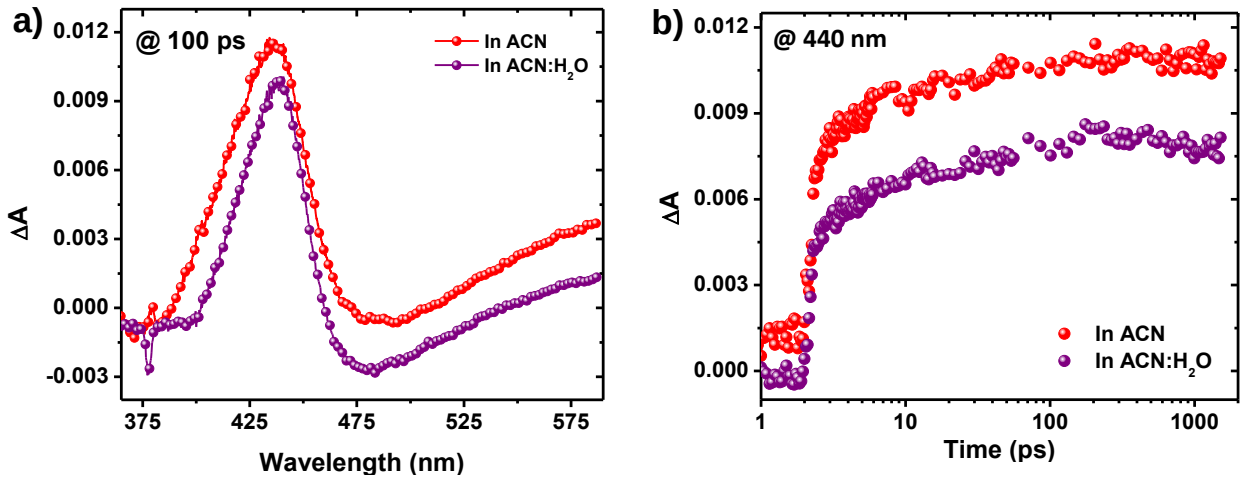


**Figure S31.** a) Transient absorption spectrum of ADD1 in ACN and ACN/Water mixture recorded at 100 ps after photoexcitation. b) Transient decay profiles of ADD1 in ACN and ACN/water mixture monitored at 440 nm following 355 nm laser excitation.

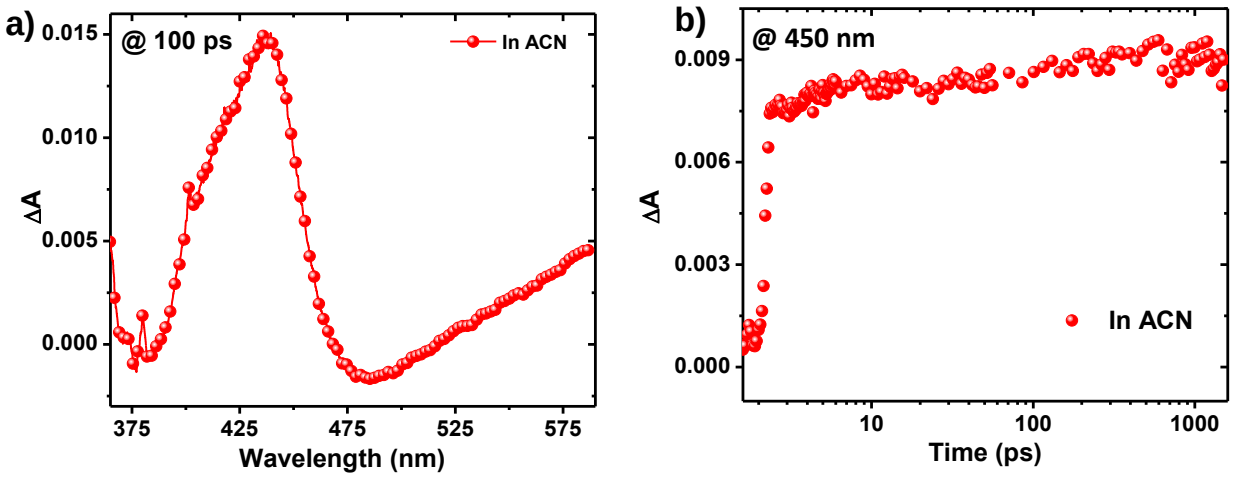


**Figure S32.** a) Transient absorption spectrum of ADDOH in ACN recorded at 100 ps after photoexcitation. b) Transient decay profiles of ADDOH in ACN monitored at 440 nm following 355 nm laser excitation.

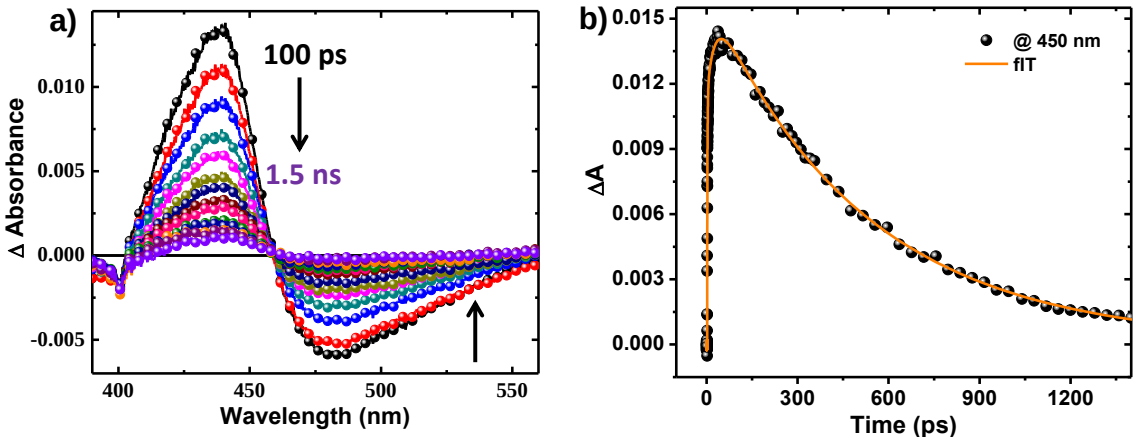


**Figure S33.** a) Transient absorption spectrum of ADDOH in ACN/Water mixture recorded at 100 ps after photoexcitation. b) Transient decay profiles of ADDOH in ACN/Water mixture monitored at 440 nm following 355 nm laser excitation.

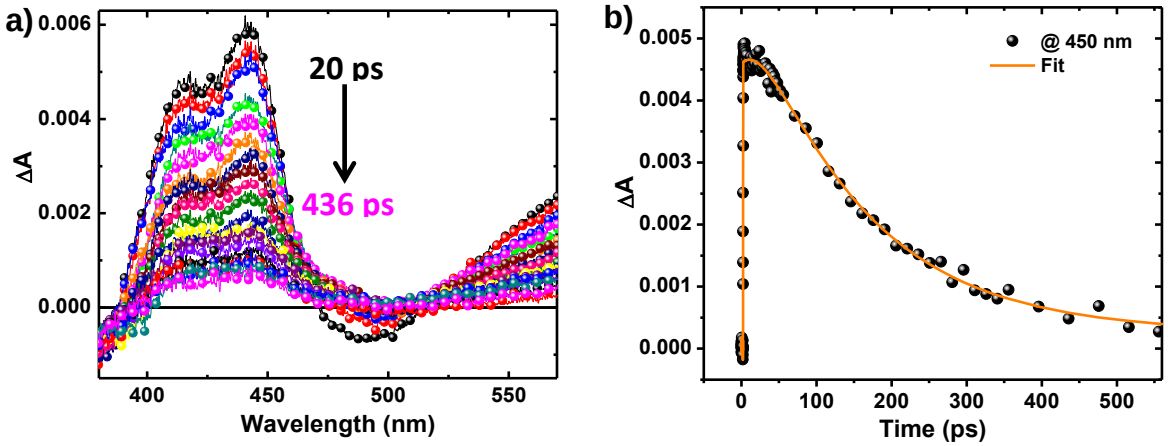


**Figure S34.** a) Transient absorption spectrum of ADDDP in ACN recorded at 100 ps after photoexcitation. b) Transient decay profiles of ADDDP in ACN monitored at 440 nm following 355 nm laser excitation.

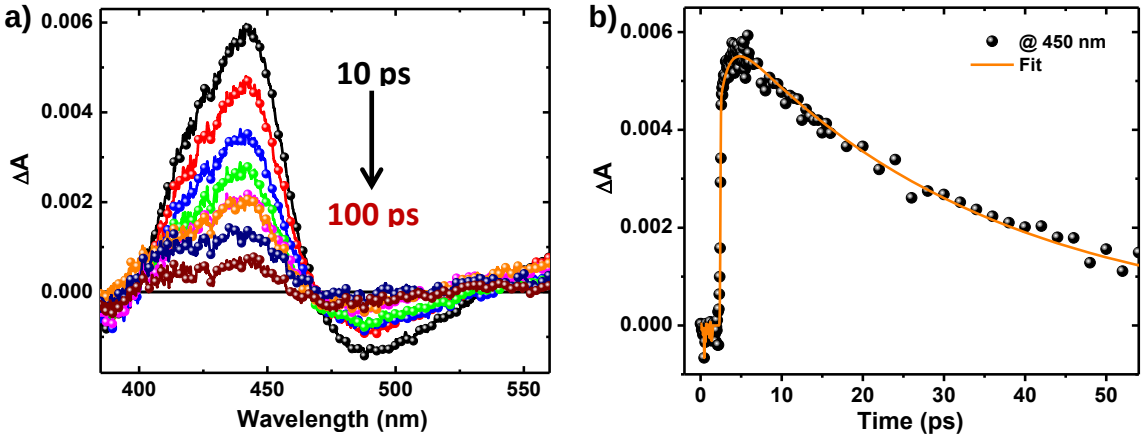


**Figure S35.** a) Transient absorption spectrum of ADDDP in ACN/Water mixture recorded at 100 ps after photoexcitation. b) Transient decay profiles of ADDDP in ACN/Water monitored at 440 nm following 355 nm laser excitation.

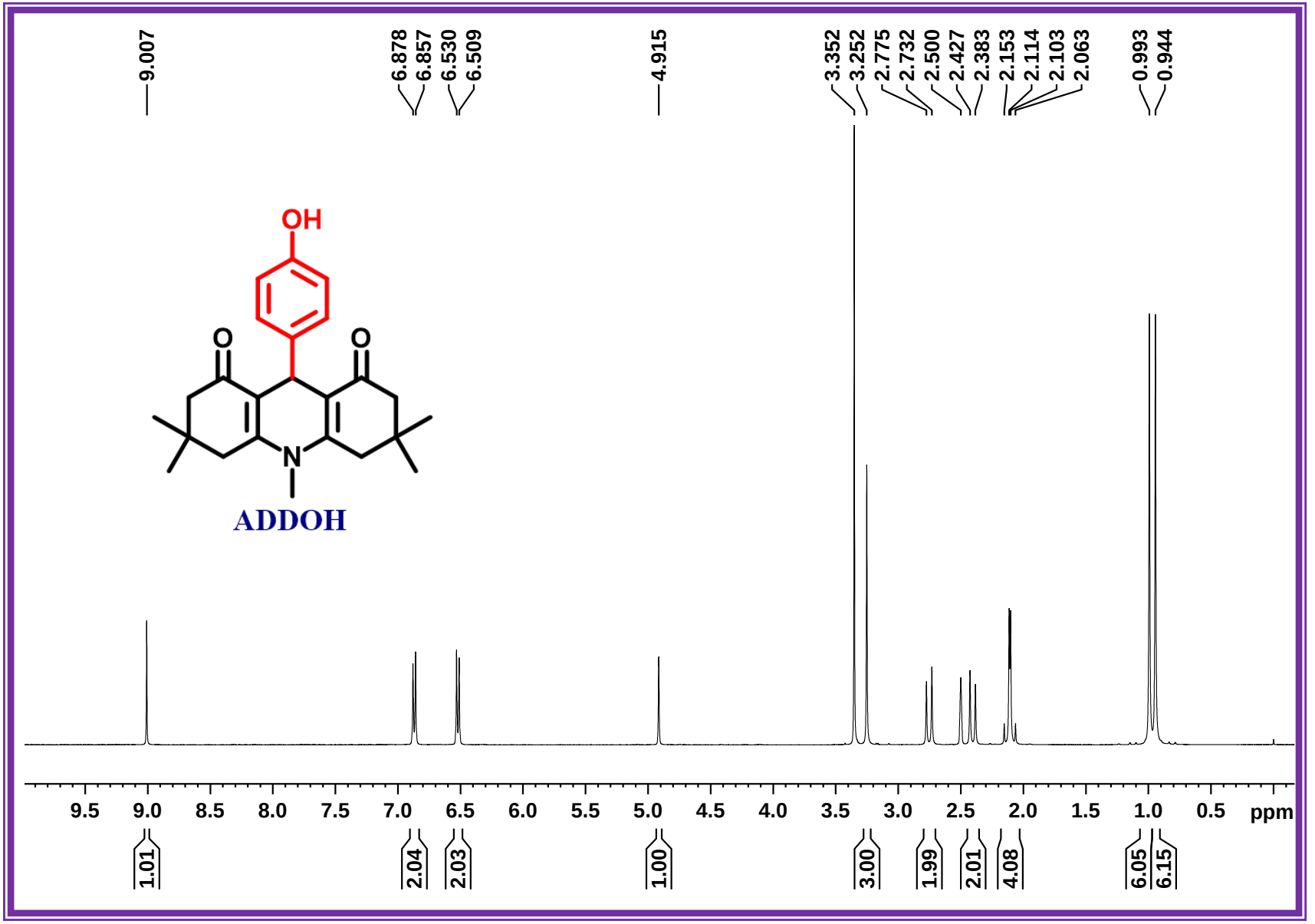


**Figure S36.** $^{1}$H NMR Spectrum of **ADDOH** in DMSO-$d_6$

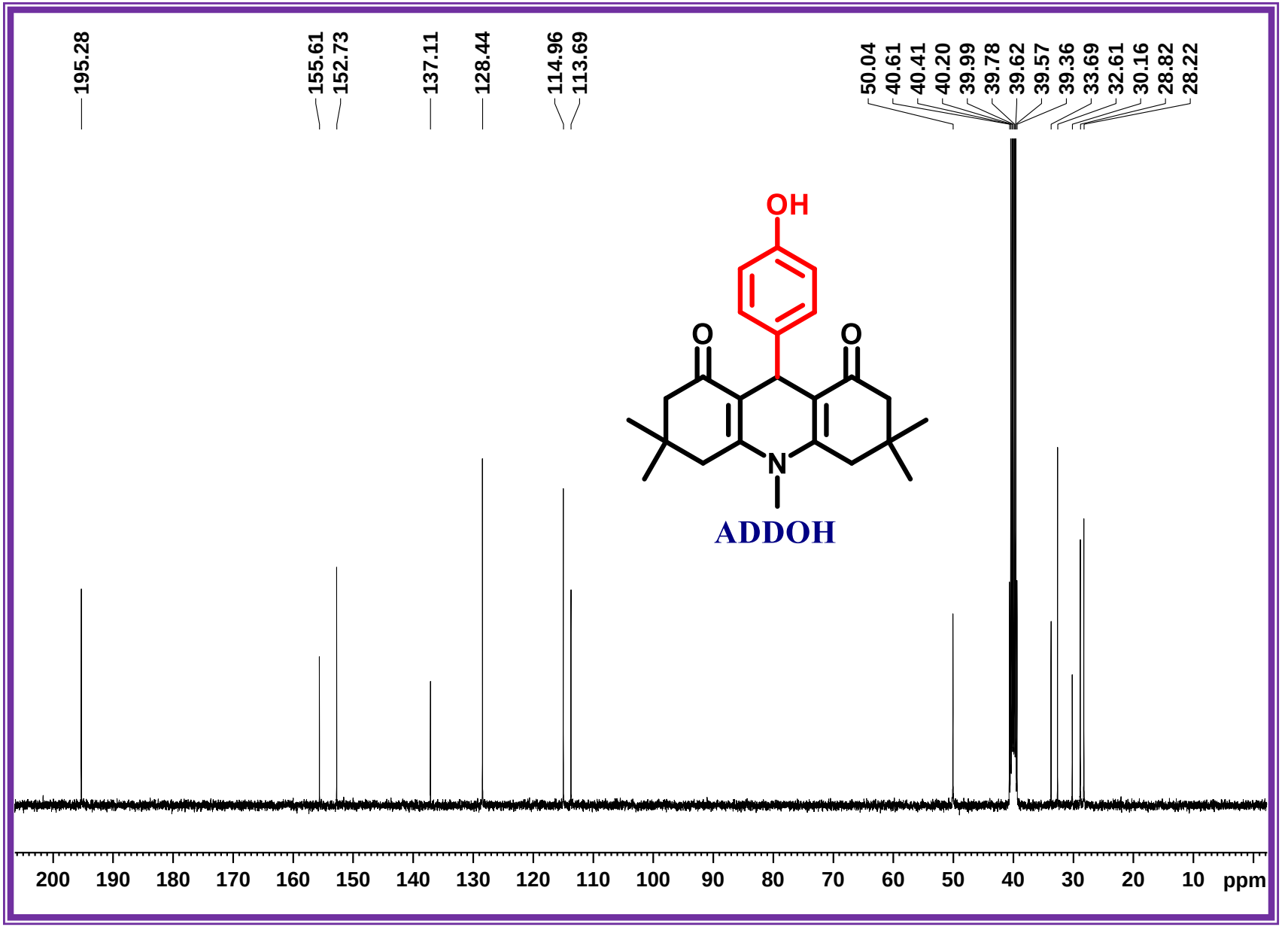


**Figure S37**. $^{13}$C NMR Spectrum of **ADDOH** in DMSO-$d_6$

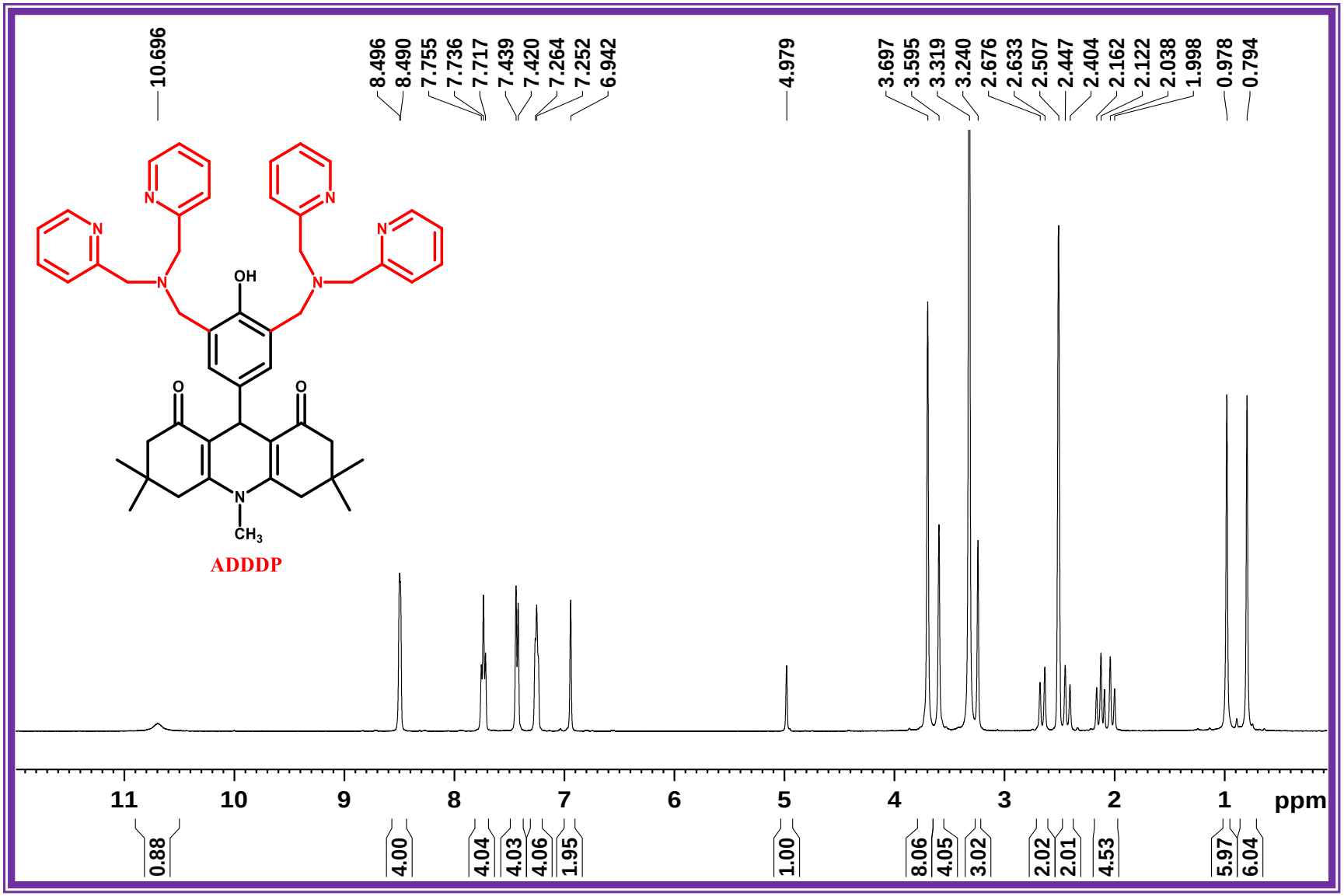


**Figure S38.** $^{1}$H NMR Spectrum of **ADDDP** in DMSO-$d_6$

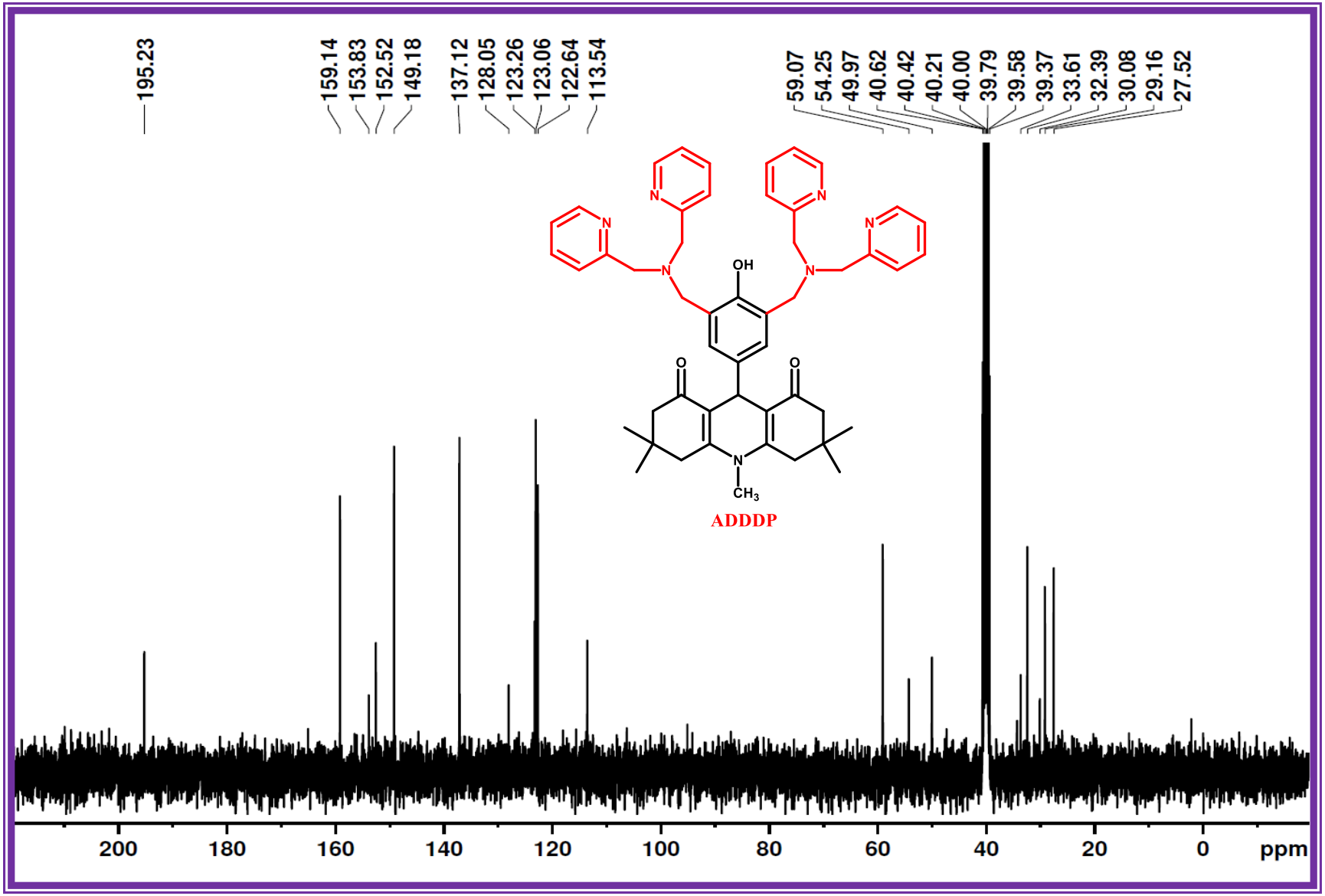


**Figure S39**. $^{13}$C NMR Spectrum of **ADDDP** in DMSO-$d_6$

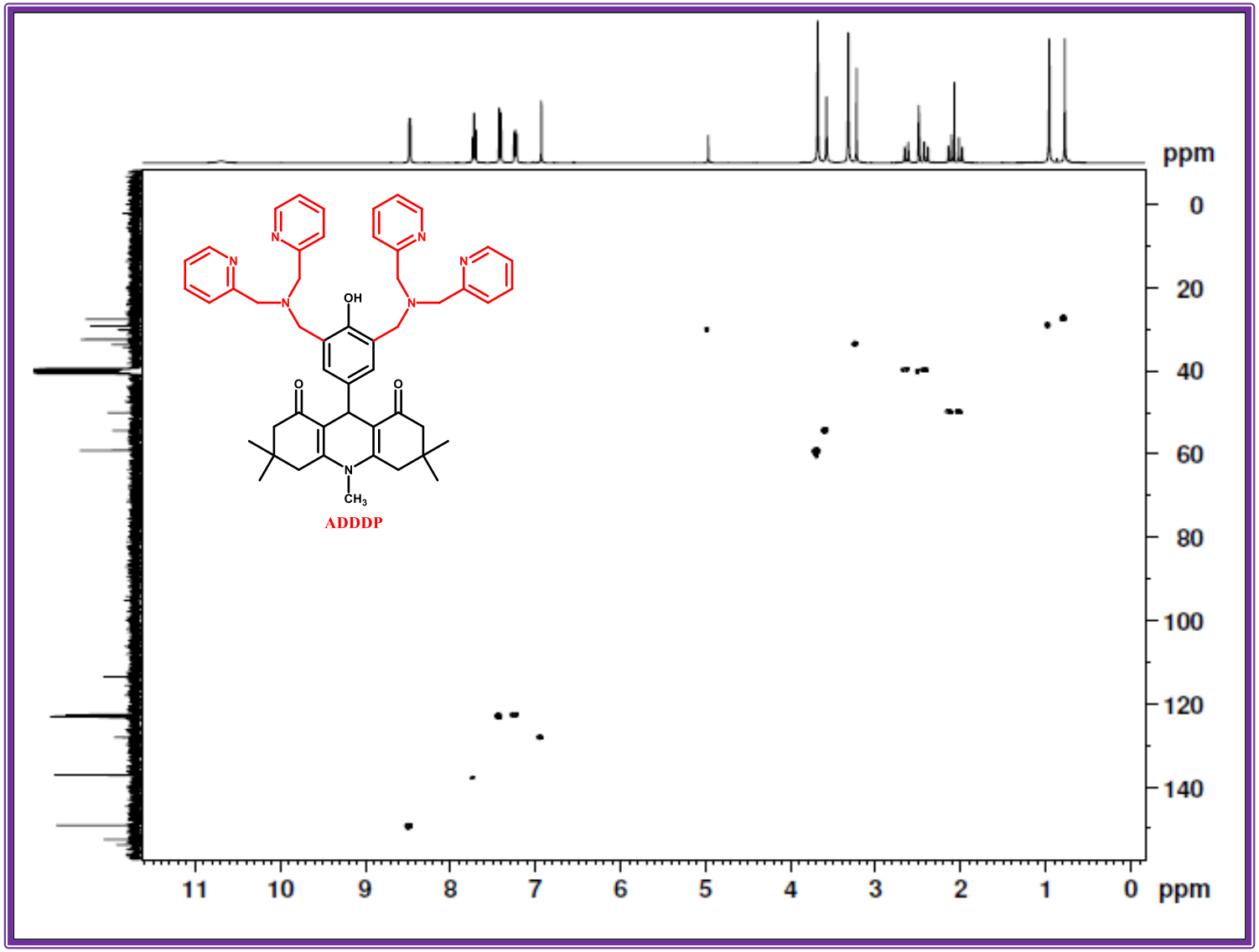


**Figure S40**. HSQC Spectrum of **ADDDP** in DMSO-$d_6$

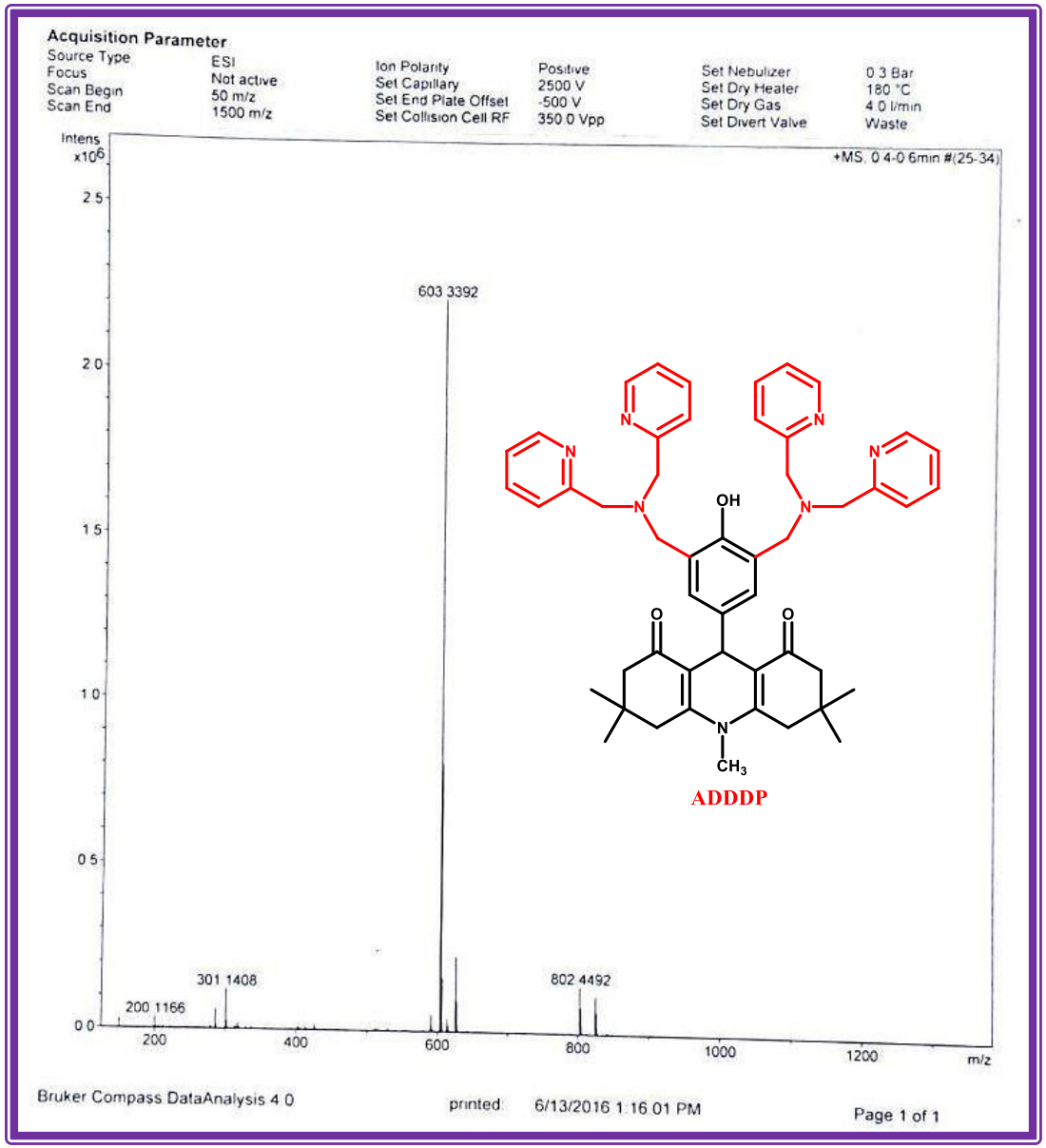


**Figure S41.** HRMS of **ADDDP**

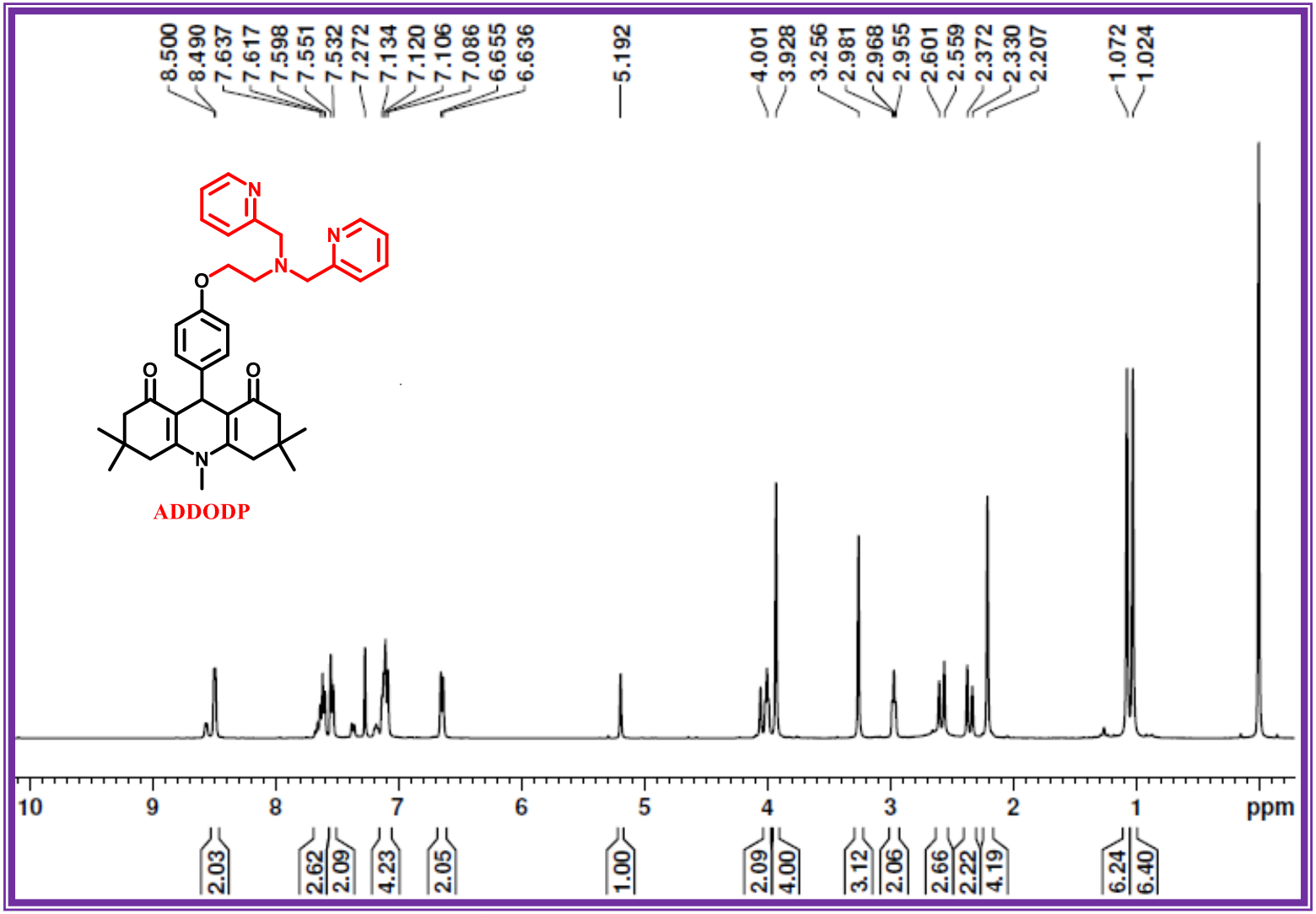


**Figure S42.** $^{1}$H NMR Spectrum of **ADDODP** in DMSO-$d_6$

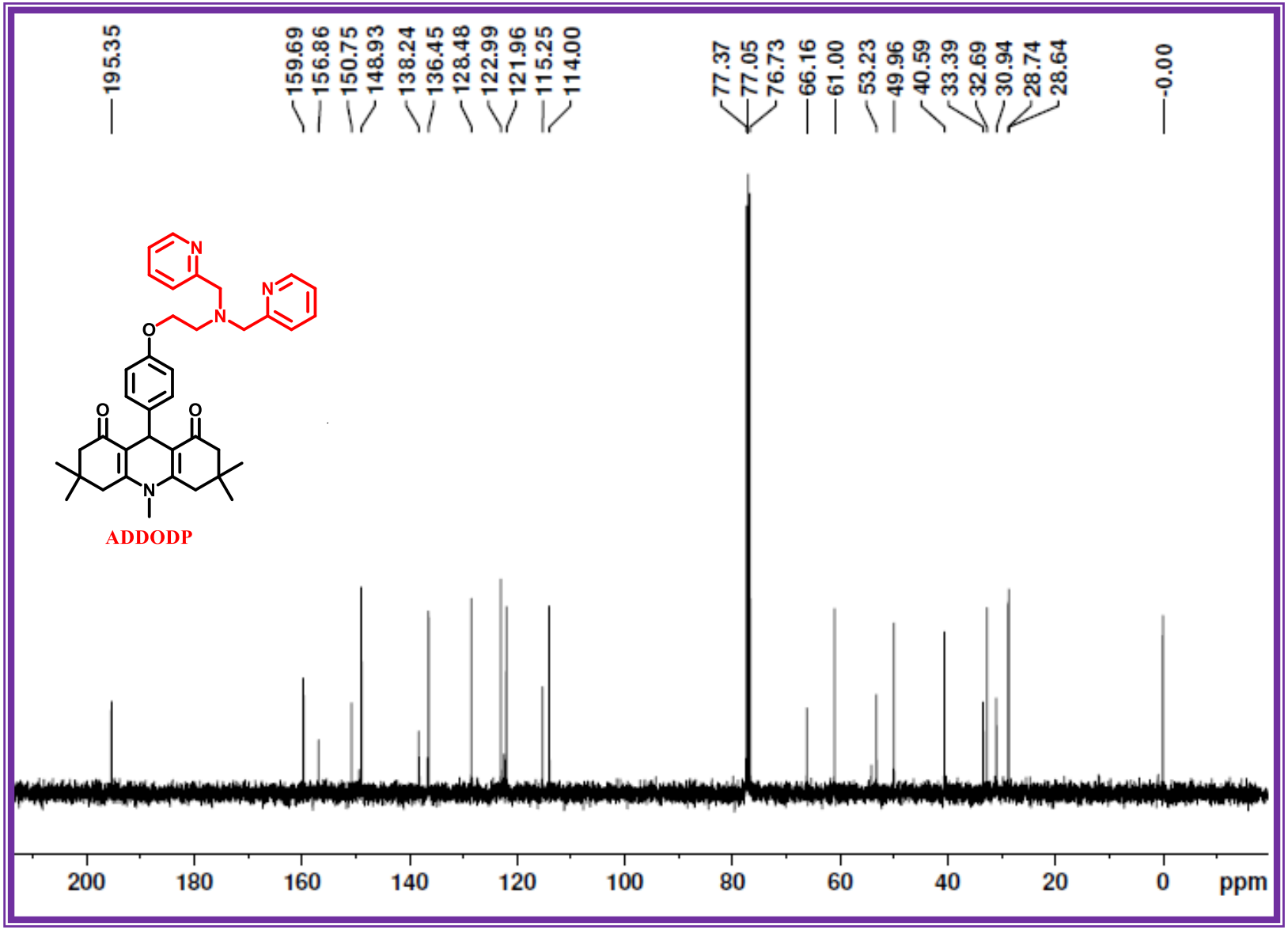


**Figure S43**. $^{13}$C NMR Spectrum of **ADDODP** in DMSO-$d_6$

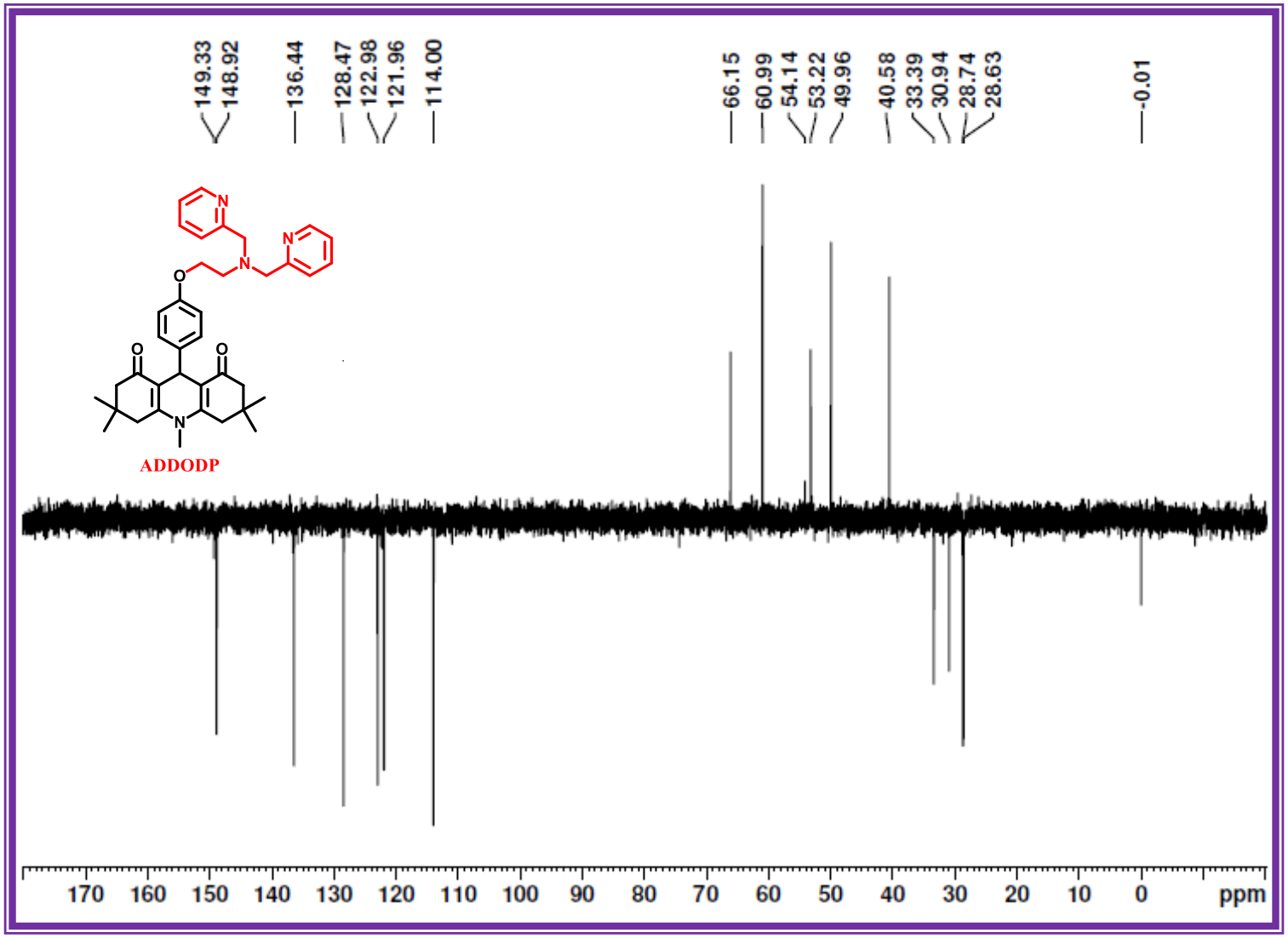


**Figure S44**. DEPT 135 Spectrum of **ADDDP** in DMSO-$d_6$

## References


1. D. Bradley, G. Williams, M. Lawton, *J. Org. Chem.*, 2010, **75**, 8351–8354.
2. W. L. F. Armarego, D. D. Perrin, *Purification of Laboratory Chemicals*, Fourth Edition, Butterworth-Heinemann, A division of Reed Educational and Professional Publishing Ltd., Oxford, 2000.
3. P. Ashokkumar, V. T. Ramakrishnan, P. Ramamurthy, *Eur. J. Org. Chem.*, 2009, 5941–5947.
4. H. Fuchida, S. Tabata, N. Shindo, I. Takashima, Q. Leng, Y. Hatsuyama, I. Hamachi, A. Ojida, *Bull. Chem. Soc. Jpn.*, 2015, **88**, 784–791.
5. R. Kumaran, P. Ramamurthy, *J. Phys. Chem. B*, 2006, **110**, 23783–23789.
6. N. Dhenadhayalan, C. Selvaraju, *J. Phys. Chem. B*, 2012, **116**, 4908−4920.
7. S. Ulrich, H. J. Timpe, J. P. Fouassier, F. Morlet-Savary, *J. Photochem. Photobio. A: Chem.*, 1993, **74**, 165–170.
8. N. Srividya, P. Ramamurthy, P. Shanmugasundaram, V. T. Ramakrishnan, *J. Org. Chem.*, 1996, **61**, 5083–5089.
9. H. Mohan, N. Srividya, P. Ramamurthy, J. P. Mittal, *J. Phys. Chem. A*, 1997, **101**, 2931–2935.
10. B. Venkatachalapathy, P. Ramamurthy, *Phys. Chem. Chem. Phys.*, 1999, **1**, 2223–2230.
11. V. Thiagarajan, C. Selvaraju, E. J. Padma Malar, P. Ramamurthy, *ChemPhysChem.*, 2004, **5**, 1200–1209.
12. V. Thiagarajan, V.K. Indirapriyadharshini, P. Ramamurthy, *J Incl Phenom Macrocycl Chem.*, 2006, **56**, 309–313.
13. P. Ashokkumar, V. T. Ramakrishnan, P. Ramamurthy, *Eur. J. Org. Chem.*, 2009, 5941–5947.
14. P. Ashokkumar, V. T. Ramakrishnan, P. Ramamurthy, *J. Phys. Chem. A*, 2011, **115**, 14292–14299.
15. R. Suresh, T. Senthil Kumar, P. Ramamurthy, *Phys. Chem. Chem. Phys.*, 2016, **18**, 32247– 32255.
16. N. Barboy, J. Feitelson, *J. Phys. Chem.*, 1984, **88**, 1065–1068.
17. P. Lu, A. M. Feinberg, G. Guirado, S. Farid, J. P. Dinnocenzo, *J. Org. Chem.*, 2014, **79**, 9297 –9304.
18. P. Gilli, L. Pretto, V. Bertolasi, G. Gilli, *Acc. Chem. Res.*, 2009, **42**, 33–44.
19. E. Raamat, K. Kaupmees, G. Ovsjannikov, A. Trummal, A. Kütt, J. Saame, I. Koppel, I. Kaljurand, L. Lipping, T. Rodima, V. Pihl, I. A. Koppel, I. Leito, *J. Phys. Org. Chem.*, 2013, **26,** 162–170.
20. I. Kaljurand, A. Kütt, L. Sooväli, T. Rodima, V. Mäemets, Ivo Leito, I. A. Koppel, *J. Org. Chem.*, 2005, **70**, 1019–1028.
21. H. Mohan, N. Srividya, P. Ramamurthy, J. P. Mittal, *J. Chem. Soc., Faraday Trans.*, 1996, **92**, 2353-2359.

**22.** H. Mohan, N. Srividya, P. Ramamurthy, J. P. Mittal, *J. Phys. Chem. A* 1997**, 101**, 2931-2935.
**23.** H. Mohan, N. Srividya, P. Ramamurthy, J. P. Mittal, *J. Phys. Chem. A* 1998**, 102**, 4444-4449.
**24.** B. Venkatachalapathy, P. Ramamurthy, *Phys. Chem. Chem. Phys*., 1999, **1**, 2223-2230.
**25.** N. Srividya, P. Ramamurthy and V. T. Ramakrishnan, *Phys. Chem. Chem. Phys*., 2000, **2**, 5120-5126.
***26.*** H. Mohan, J. P. Mittal, *Journal of Photochemistry and Photobiology A: Chemistry* 2001,**141**, 25–32.
**27.** V. Thiagarajan, C. Selvaraju, P. Ramamurthy, *Journal of Photochemistry and Photobiology A: Chemistry* 2003, **157,** 23–31.
**28.** C. Selvaraju, P. Ramamurthy, *Chem. Eur. J.* 2004, **10**, 2253 - 2262.
**29.** M. Sjödin, S. Styring, B. Åkermark, L. Sun, L. Hammarström, *J. Am. Chem. Soc.*, 2000, **122**, 3932–3936.